Systematic Assessment of a Maxilla of *Homo* From Hadar, Ethiopia

WILLIAM H. KIMBEL,[1]* DONALD C. JOHANSON,[1] AND YOEL RAK[1,2]
[1]*Institute of Human Origins, Berkeley, California 94710*
[2]*Department of Anatomy, Sackler Medical School, Tel Aviv University, Tel Aviv, Israel*

KEY WORDS Pliocene hominids; palatofacial morphology; dentition

ABSTRACT The Hadar site in Ethiopia is a prolific source of hominid fossils attributed to the species *Australopithecus afarensis*, which spans the period 3.4–3.0 million years (myr) in the Sidi Hakoma, Denen Dora and lower Kada Hadar Members of the Hadar Formation. Since 1992 a major focus of field work conducted at Hadar has centered on sediments younger than 3.0 myr, comprising the bulk of the Kada Hadar Member. Witnessing the rise of the "robust" *Australopithecus* clade(s), the origin of *Homo*, and the first record of lithic artifacts, the period between 3.0 and 2.0 myr is strategically vital for paleoanthropology. However, in eastern Africa it is a particularly poorly sampled temporal interval.

This paper provides a detailed comparative description of a hominid maxilla with partial dentition found at Hadar in 1994. The specimen, A.L. 666-1, derives from a lithic artifact–bearing horizon high in the Kada Hadar Member, 0.8 m below the BKT-3 tephra, dated by the $^{40}Ar/^{39}Ar$ method to 2.33 ± 0.07 myr. Our preliminary investigation of the hominid specimen showed unambiguous affinities with early representatives of the *Homo* clade (Kimbel et al. [1996] J. Hum. Evol. *31:*549–561). Further studies on maxillary and dental morphology lead us to attribute A.L. 666-1 to *Homo* aff. *H. habilis*. The new Hadar jaw is the first paleontological evidence for the projection of the *H. habilis* maxillofacial morphotype well back into the Pliocene. It may represent a male of this species, whose maxillary hypodigm consists chiefly of females. A subsidiary finding of our study is that of the three earliest recorded species of *Homo* (*H. habilis, H. rudolfensis, H. erectus*), it is *H. habilis* that exhibits facial morphology closest to that expected in their last common ancestor. Am J Phys Anthropol 103:235–262, 1997.

The Ethiopian site of Hadar is renowned for its rich yield of Pliocene vertebrate fossils, including numerous, well preserved remains of Hominidae. Early work at Hadar, carried out by the International Afar Research Expedition from 1973 to 1976, added significantly to the understanding of human evolution during the middle Pliocene, at a time when the hominid record older than 3 million years (myr) ago was a virtual void. The identification of the species *Australopithecus afarensis* by Johanson et al. (1978) relied heavily on the Hadar hominid sample, which by 1977 comprised 250 specimens, and promoted refreshed debate on early hominid systematics and paleobiology that

Contract grant sponsor: National Science Foundation; contract grant number SBR 8820113; contract grant number SBR 9222604; contract grant number SBR 9511172; contract grant sponsor National Geographic Society.

*Correspondence to: William H. Kimbel, Institute of Human Origins, 1288 Ninth St., Berkeley, CA 94710. E-mail: whk@iho.org

Received 18 September 1996; revised 25 March 1997; accepted 27 March 1997.

is ongoing 18 years after Johanson and White's (1979) "A Systematic Assessment of Early African Hominids."

Beginning in 1990 Hadar has been the locus of paleoanthropological and geological field research conducted by the Institute of Human Origins under the auspices of the Center for Research and Conservation of Cultural Heritage (Ethiopian Ministry of Information and Culture). Four field seasons have resulted in further additions to the hominid record in refined geochronologic and paleoenvironmental contexts (Kimbel et al., 1994; Renne et al., 1993; Walter and Aronson, 1993; Walter, 1994). Through December 1994 the total Hadar hominid inventory stands at 332 specimens.

Prior to 1992 *A. afarensis* in the Hadar Formation was all but confined to the Sidi Hakoma Member and the overlying Denen Dora Member, which together constitute roughly the lower 50% of the formation's thickness north of the Awash River in the eastern part of the Hadar site. This stratigraphic interval is bracketed by tephra dated to 3.4 and 3.18 myr ago (Walter and Aronson, 1993; Walter, 1994; see Fig. 1). The Kada Hadar Member, comprising the sedimentary package stratigraphically above the Kada Hadar Tuff (3.18 myr), was poorly known paleontologically and geologically, although Oldowan lithic artifacts have been recovered from both primary and secondarily derived contexts within this member's youngest deposits in the Gona drainage since the mid-1970s (Corvinus, 1976; Roche and Tiercelin, 1977; Harris, 1983; Semaw et al., 1997). As an illustration of the biased paleontological documentation of the Hadar Formation through the 1970s, consider that from 1973 to 1976 only two of 28 (ca. 7%) hominid localities were known from sediments above the Kada Hadar Tuff.

It is now clear that the time period between 3.0 and 2.0 myr is a particularly momentous one in hominid evolution, witnessing the rise of the "robust" *Australopithecus* clade(s) as well as the origin of our own. Yet the hominid paleontological record over most of this time period in eastern Africa is poor (Kimbel, 1995; White, 1995). Thus, beginning in the 1992 field season, paleontological and geological field work at Hadar took a strategic turn toward the upper deposits in the Hadar Formation, those younger than 3.18 myr. Of the 35 new hominid-bearing localities identified in 1990–1994, 11 (ca. 31%) sample Kada Hadar Member deposits. Hominid fossils from these localities include the youngest known *A. afarensis* specimens and the first fairly complete adult skull of this species (Kimbel et al., 1994), which are situated 10–12 m stratigraphically below the BKT-2 tephra complex, dated to 2.95 myr (Fig. 1).

Sediments stratigraphically above the BKT-2 complex were completely unknown paleontologically until 1993, when several locally rich but dispersed faunal concentrations sampling "upper" Kada Hadar Member sediments were identified in both the eastern and western sectors of the Hadar site. In 1994 these areas were targeted for intensive paleontological survey, leading to the first ever discovery of hominid remains in Hadar Formation sediments younger than 3.0 myr old.

Among the latter discoveries, the most important is a maxilla with partial dentition (A.L. 666-1) found in close proximity to Oldowan stone artifacts on the surface of "upper" Kada Hadar Member deposits in the Makaamitalu drainage of the Awash River's Kada Hadar tributary, about 1.2 km upstream from *A. afarensis* skull locality A.L. 444 (Kimbel et al., 1994). We have elsewhere summarized the circumstances of the specimen's recovery, the preliminary evidence for its late Pliocene geological age and archeological associations, and its morphological affinities with *Homo* (Kimbel et al., 1996), which we briefly review below. The present communication follows up with a thorough anatomical description and comparative systematic analysis of the hominid specimen.

STRATIGRAPHIC CONTEXT, AGE AND ASSOCIATIONS

The deposits in the Makaamitalu basin occur stratigraphically above a disconfor-

Fig. 1. Schematic stratigraphic section of the Hadar Formation, showing selected hominid localities and radioisotopic ages (see Walter, 1994; Walter and Aronson, 1993; Renne et al., 1993; Kimbel et al., 1996). The A.L. 666-1 hominid specimen is sited stratigraphically 0.8 m below the BKT-3 tephra. Intraformational member boundaries indicated at left.

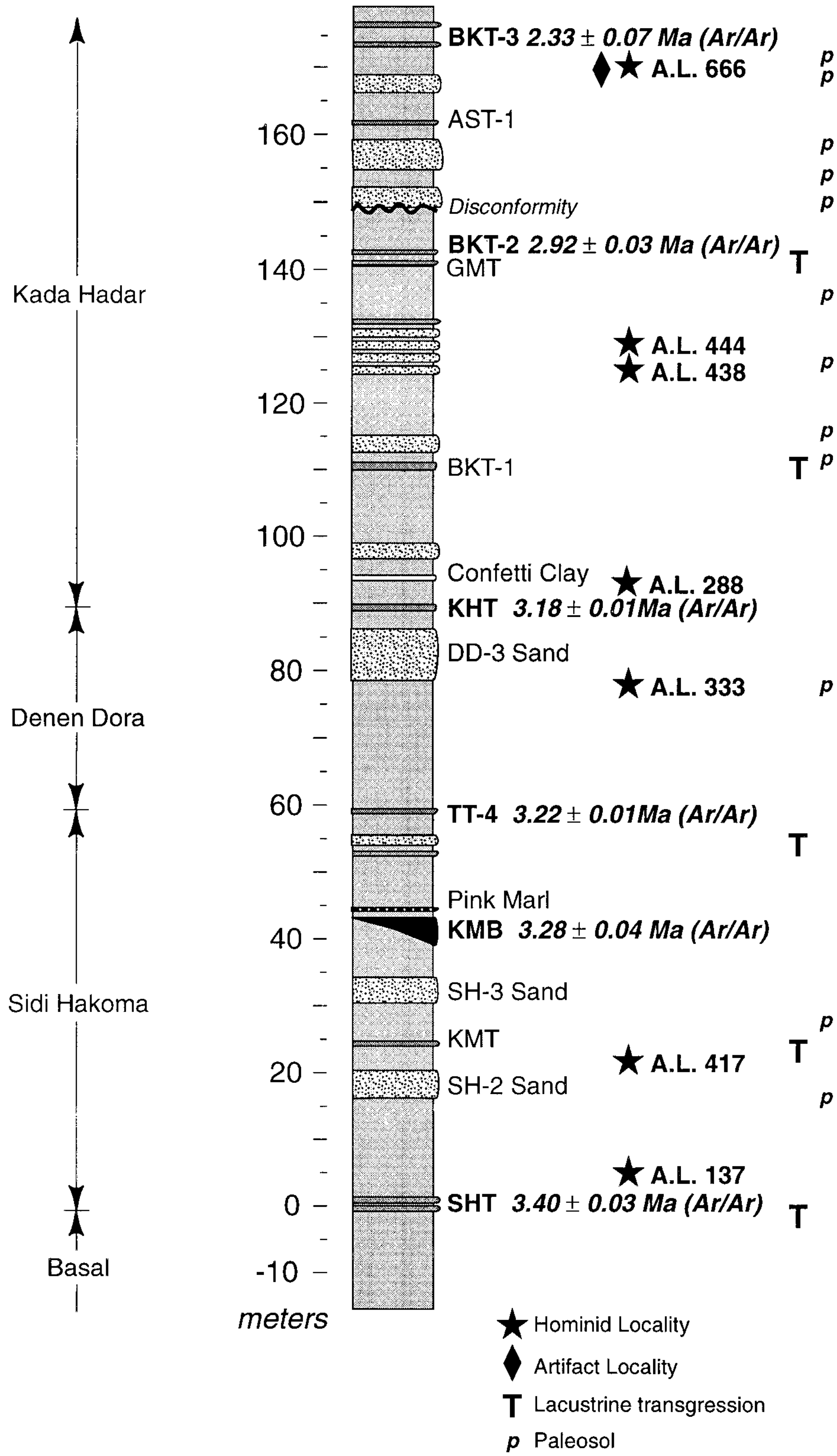

BKT-3 2.33 ± 0.07 Ma (Ar/Ar)
A.L. 666
AST-1
Disconformity
BKT-2 2.92 ± 0.03 Ma (Ar/Ar)
GMT
A.L. 444
A.L. 438
BKT-1
Confetti Clay
A.L. 288
KHT 3.18 ± 0.01Ma (Ar/Ar)
DD-3 Sand
A.L. 333
TT-4 3.22 ± 0.01Ma (Ar/Ar)
Pink Marl
KMB 3.28 ± 0.04 Ma (Ar/Ar)
SH-3 Sand
KMT
A.L. 417
SH-2 Sand
A.L. 137
SHT 3.40 ± 0.03 Ma (Ar/Ar)
Kada Hadar
Denen Dora
Sidi Hakoma
Basal
160
140
120
100
80
60
40
20
0
-10
meters
p
T
Hominid Locality
Artifact Locality
Lacustrine transgression
Paleosol

Fig. 1.

mity in the upper part of the Kada Hadar Member (ca. 60 m above the Kada Hadar Tuff; see Fig. 1). Evidence from sedimentology and vertebrate paleontology concordantly suggest a marked shift at Hadar to drier, more open habitats above the disconformity due to climatic and/or tectonic factors (Kimbel et al., 1996). A.L. 666 is a hill composed of a 3.5 m thick siltstone situated stratigraphically 10–15 m above the disconformity and 0.8 m below the tephra known as BKT-3, whose type-locality outcrops in the Makaamitalu basin (Fig. 1). Single-crystal laser fusion (SCLF) $^{40}Ar/^{39}Ar$ dating by R.C. Walter of low K-content plagioclase crystals indicate an eruptive age for BKT-3 of 2.33 $\pm$ 0.07 myr, agreeing with a fission-track age of 2.3 $\pm$ 0.5 myr (Walter, 1989) and biochronologic pointers from the Makaamitalu basin mammalian assemblage (Kimbel et al., 1996). As the likely source horizon for both the hominid fossil and the artifacts at A.L. 666 is correlated stratigraphically to less than 1 m below BKT-3, 2.33 myr is the *minimum* age for the A.L. 666-1 maxilla. This is a poorly sampled time period in the African hominid fossil record (Feibel et al., 1989, 1991; Kimbel, 1995; White, 1995).

The hominid maxillary fragments and isolated dental elements belonging to them were recovered from the surface at A.L. 666 closely associated with fresh-appearing Oldowan flakes and bifacially flaked "end-choppers." A small trial excavation conducted during the 1994 field season led to the recovery of 14 in situ lithics (including a conjoining flake and core) as well as three nonhominid mammal bone fragments (Kimbel et al., 1996). Details of recovery and preservation leave little doubt as to the derivation of the hominid specimen from the artifact-bearing siltstone horizon at A.L. 666.

MATERIALS AND METHODS

For this study we compared A.L. 666-1 to a broad range of hominid fossil maxillae (originals, or casts where noted) assigned to *Australopithecus* (including *Paranthropus* of some authors) and *Homo*. The relevant hypodigms are:

Australopithecus afarensis: Hadar Formation (stratigraphically below the BKT-2 tephra), Ethiopia (A.L. 199-1, 200-1, 333-1, 333-2, 413-1, 417-1, 427-1, 442-1, 444-2, 486-1, 651-1; plus isolated and/or associated teeth); Garusi I plus isolated and/or associated teeth from the upper Laetolil Beds, Tanzania.

Australopithecus africanus: Sterkfontein, Member 4 ("Type Site") (TM 1511, 1512, 1514, Sts. 5, 17, 52, 53, 71, Stw. 13, 73, cast of Stw. 505; plus isolated and/or associated teeth) and Makapansgat, Member 3 (MLD 6/23, 9, 45).

Australopithecus aethiopicus: cast of KNM-WT 17000 from the Lomekwi Member, Nachukui Formation, Kenya.

Australopithecus robustus (including *A. crassidens* of some authors): "robust" hominid fossils from Kromdraai (TM 1517) and Swartkrans (SK 11, 12, 13, 46, 48, 52, 55, 65, 79, 83, SKW 11, 29, SKX 265, plus isolated and/or associated teeth).

Australopithecus boisei: "robust" hominid fossils from Member G, Shungura Formation, Ethiopia (Omo 323-76-896); Olduvai Gorge, Bed I, Tanzania (O.H. 5); KBS and Okote Members, Koobi Fora Formation, Kenya (KNM-ER 405, ER 406, ER 732, ER 733, plus isolated and/or associated teeth).

Homo habilis: Upper Burgi Member and base of KBS Member, Koobi Fora Formation (KNM-ER 1805, ER 1813, ER 3891); Bed I through lower middle Bed II, Olduvai Gorge (O.H. 13, O.H. 16, O.H. 24, O.H. 62, plus isolated and/or associated teeth discussed and/or tabulated below); Member G, Shungura Formation (L. 894-1); Sterkfontein, Member 5 (Stw. 53). For the East African material, this closely follows the assignments of Wood (1993) with the exception of KNM-ER 3891, which is attributed by him to *H. rudolfensis.*

Homo rudolfensis: Upper Burgi Member, Koobi Fora Formation (KNM-ER 1470, ER 1590).

Homo erectus: KBS Member, Koobi Fora Formation (KNM-ER 807, ER 1808, cast of ER 3733); Natoo Member, Nachukui Formation (cast of KNM-WT 15000); Swartkrans, Member 1 (SK 27, SK 847); Pucangan Formation, Indonesia (cast of Sangiran 4); Zhoukoudian Lower Cave, China (casts of Z. D-I, F-IV, L-I, L-II, O-I, plus isolated teeth from Weidenreich, 1937). The composition of this

hypodigm is likely to provoke disagreement, as we do not here recognize *H. ergaster* (for KNM-ER 3733 and WT 15000), per Wood (1991, 1993) and others (e.g., Clarke, 1994); nor do we delete SK 847, as recently argued by Grine et al. (1993) on morphometric grounds (its phenetic affinities, they find, lie with *H. habilis*, particularly Stw. 53). We have elsewhere (Kimbel and Rak, 1993) summarized the difficulties with the phylogenetic individuation of separate "early" African and Asian clades within the *H. erectus* hypodigm. We refer readers there, but especially to the following, for details: Rightmire (1991); Harrison (1993); Walker (1993); Bräuer (1994). On the taxonomic placement of SK 847, we conclude that this cranium exhibits more derived states in the degree of nasal bridge projection, the conformation of the supraorbital torus and the basal morphology of the temporal bone than does *H. habilis* (as delineated above). We see no morphological (as opposed to morphometric) evidence for the attribution of SK 847 to the species represented by fossils such as KNM-ER 1813, O.H. 24 and Stw. 53.

Dental metric comparisons reported here are based on samples discussed and tabulated in White et al. (1981), augmented as noted in the tables below. All measurements in the descriptions are in millimeters.

The hominid maxilla

Preservation. At the time of discovery, the hominid maxilla was in two major pieces comprising the left and right halves, broken cleanly along the intermaxillary suture. The left half retained P^3 and P^4 crown fragments and the roots of M^1; the right half held P^3-M^1 crowns plus M^2-M^3 roots. Intensive surface collecting followed by dry-sieving at A.L. 666 resulted in the recovery of approximately 30 tooth crown, tooth root and maxillary bone fragments, including LI^2 with root, two lingual fragments of LC crown with root, three fragments of RC crown, three fragments of LP^3 crown and root, eight pieces of LP^4 crown and root, two small pieces of lingual alveolar marginal bone at $LM^{1/2}$, three fragments of LM^1 crown and root, four pieces of LM^2 root system and M^3 alveolar bone, four fragments of LM^2 crown, and a small fragment of posterolateral maxillary sinus wall from the right side. All of these pieces, save the RC crown portion, fit cleanly on to the main portions of the maxilla.

The specimen is well preserved, undistorted, and most breaks are fresh. On each side the frontal process is missing and the zygomatic process is represented by its roots only. The maxillary sinus cavities and nasal cavity are well preserved. The palate surface is intact posteriorly to the M^2/M^3 level. Most of the labial/buccal alveolar bone on the left side is broken away, revealing the LC root and buccal postcanine tooth roots; loss of labial alveolar bone exposes the (empty) RC and LI^1 alveoli; lingual alveolar bone is lost at LM^2 but is otherwise intact.

Of the dentition, RP^3–M^1 are intact as found in the jaw; the broken, weathered roots of RM^2–M^3 probably indicate prefossilization loss of their crowns. Although there is a match between the distal interproximal facet (IPF) of RC and the mesial IPF of RP^3, an insufficient amount of the canine root remains to permit the fitting of the crown in the alveolus. On the left side, partial or full crowns of I^2–M^2 are present. The LI^2 is complete; LC lacks the distolabial quadrant; LP^3 is missing about two-thirds of its buccal aspect plus a small wedge from its lingual aspect; LP^4 lacks the middle one-third of its mesial aspect; LM^1 is missing most of the mesiolingual corner; LM^2 is intact. The empty LM^3 alveolus was matrix filled, indicating prefossilization loss of this tooth.

Morphology

Facial aspect (Fig. 2). The maxilla is deep, broad and square in anterior view. There is no superomedial tapering of the midfacial portion of the maxilla from the canines' alveolar margins to the lateral margins of the nasal aperture. The nasoalveolar clivus is long, modestly prognathic, and flat sagittally as well as transversely, except over the empty central incisor alveoli where pronounced jugae reflecting labially convex incisor roots swell the (broken) labial alveolar plates and gently round the clivus in both planes. The direct nasospinale-prosthion chord is 32, but the horizontal projected distance between these points constitutes only 63% of the direct measure, reflecting

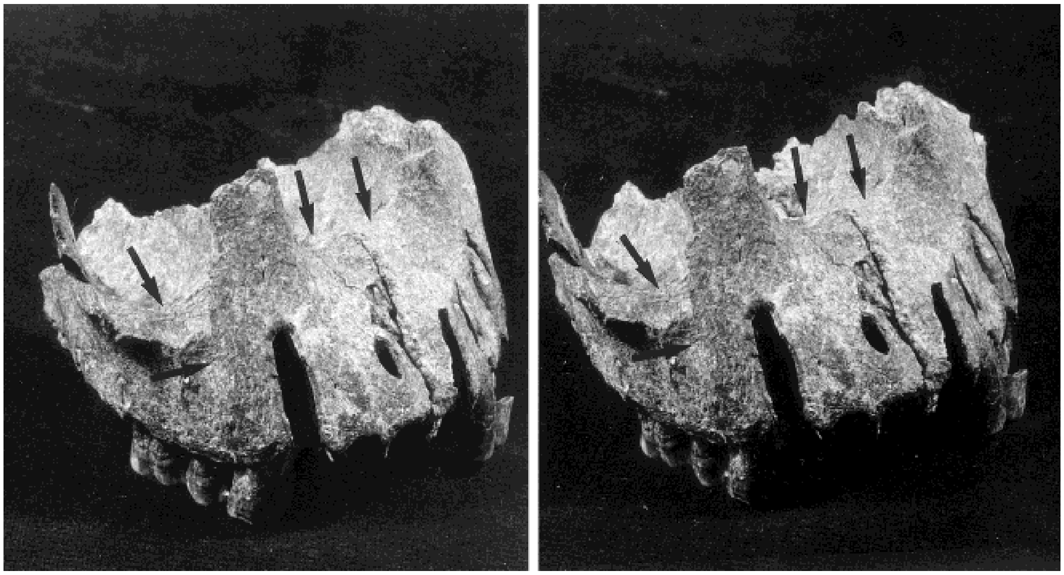

Fig. 2. Superior oblique view of A.L. 666-1, stereoscopic pair (90% of natural size). Arrows indicate (clockwise from lower left): rudimentary canine fossa, with vertical, anterior limiting crest above P^3 jugum; anterior septum in floor of right maxillary sinus; elevated intranasal platform; inferior margin of nasal cavity. See text for comparative discussion of these characters.

the relative verticality of the clivus and the absence of strong subnasal prognathism. From its intact palatal margin to the apex the empty LI^1 alveolus measures 16.2 deep, or about 50% of the vertical height of the nasoalveolar clivus.

The anterior maxillary surface adjacent to the nasal aperture is flat and directed anteriorly and slightly laterally, resulting in weak eversion of the aperture's lateral margins. Faint extensions of these margins (*cristae lateralis*) curve inferomedially on the nasoalveolar clivus, creating a slight recess of the upper quarter of the clivus and inferior nasal margin behind the plane of the aperture. The inferior corners of the nasal aperture are tightly curved in horizontal cross-section, but owing to the recess they are not sharp. Maximum breadth of the nasal aperture is 24, measured just above the level of the inferior corners. At the entrance of the aperture sits a strong, tuberclelike anterior nasal spine, which is split into two moieties by the intermaxillary suture and from which a weak median crest runs inferiorly on the nasoalveolar clivus for 8.0 before fading into the general bone surface.

Lateral aspect (Figs. 2, 3A,B). The upper half of the nasoalveolar clivus is straight in lateral profile, whereas the lower half is mildly convex labially, due to the curvature of the incisor roots. The convex part of the clivus projects weakly anterior to the canines. The clivus makes a strong angle (ca. 50°; see Medial Aspect, below) with the external alveolar line but the anterior maxillary surface adjacent to the nasal aperture rises at a much steeper angle, about 65° relative to the alveolar line, indicating a relatively upright superior midface. The anterior maxillary surface is bounded laterally by a thin, sharp, vertical crest that interrupts the otherwise featureless transition to the lateral facing portion of the maxilla. This crest arises 22 above the P^3 alveolar margin and runs posterosuperiorly for 9. Between the crest and the anterior root of the zygomatic process is a very shallow, 4 wide, tear-drop shaped depression—a rudimentary canine fossa—that comprises the entirety of the lateral-facing maxillary surface between the frontal and zygomatic processes. The topographic passage to the zygomatic process is very gradual, the anterior surface of the maxilla diverging from the

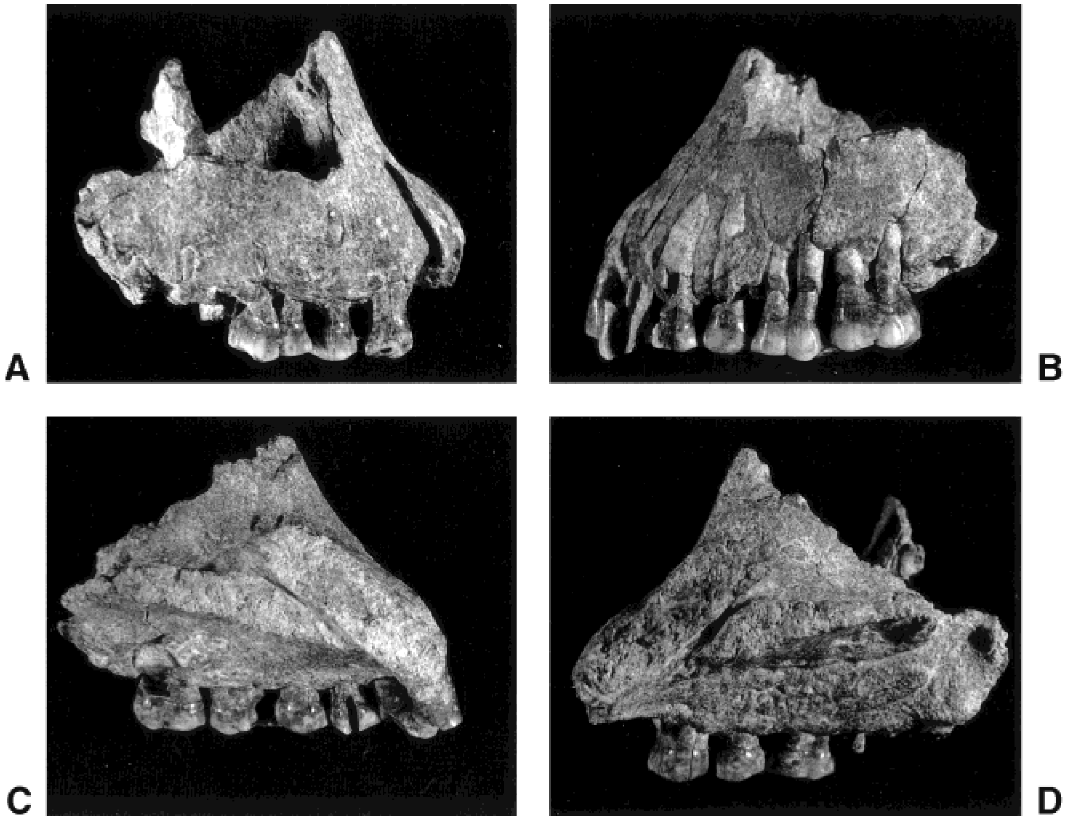

Fig. 3. A.L. 666-1: right lateral (**A**), left lateral (**B**), medial view of left side (**C**), medial view of right side (**D**). Eighty-two percent of natural size.

sagittal plane along a smooth, externally convex arc beginning anteriorly above the middle of P^4. The inferior margin of the zygomatic process root is inflated by the maxillary sinus and evenly curved. The lowest point on this margin lies 13 above the alveolar margin at the level of M^1/M^2.

Medial aspect (Figs. 3C,D). The midsagittal section of the nasoalveolar clivus (i.e., the nasospinale-alveolare line) is set at an angle of 49° to the alveolar plane. It is more or less uniformly thick, measuring 9.0 perpendicular to its long axis, and overlaps the palatine process of the maxilla extensively (9.5). The angle between the clivus and the posteroinferiorly inclined anterior floor of the nasal cavity is nearly acute. Thickness of the palatine process is maximum (7.0) in the coronal plane of the incisive canal's nasal orifice. It tapers quickly both anteriorly and posteriorly from this point, and has a strong anteroinferior to posterosuperior inclination, resulting in a progressive posterior divergence from the alveolar process and thus a marked deepening of the palate to the rear.

Superior aspect (Fig. 4A). The maxilla has a short, broad appearance in this aspect. Transverse breadth across the lateralmost preserved points on the outer maxillary sinus walls is 79. The sinus cavities are extensive, reaching anteriorly to occupy the same coronal plane as the inferior margin of the nasal aperture and laterally to invade the roots of the zygomatic processes. They are D-shaped and are widest at their anteroposterior midpoints, above M^1/M^2. Each sinus floor is divided into a large, deep posterior chamber and a small, shallow anterior chamber by a prominent, anteromedial

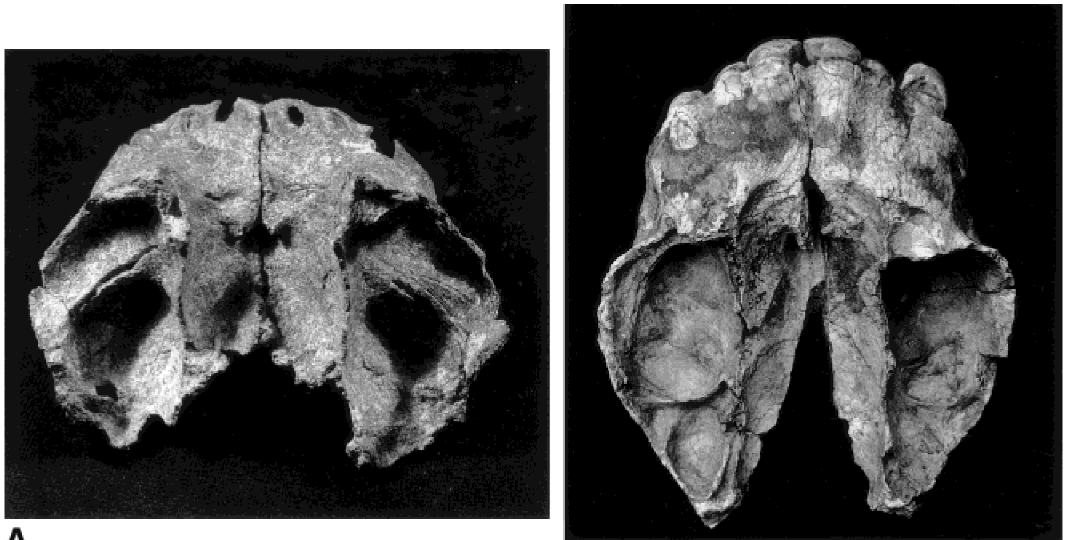

Fig. 4. Superior views, A.L. 666-1 (**A**) and *A. afarensis* maxilla A.L. 200-1a (**B**). Seventy-six percent of natural size. See text for comparative discussion of subnasal prognathism, the topography of the nasal cavity, and the morphology of the maxillary sinus antrum.

to posterolateral oriented partition. Along the crest of the partition runs a strong sulcus for the superior alveolar nerve and vessels. The anterior chamber extends laterally into the root of the zygomatic process. The thin floor of each posterior cavity bears strong impressions for the lingual root of M^2 and the mesiobuccal roots of M^2 and M^3; the latter perforates the floor on the left side.

The inferior nasal margin marks a sharp, strongly angled transition between the naso-alveolar clivus and the anterior part of the nasal cavity floor. The margin is in the form of a distinct *crista spinalis* extending laterally from the anterior nasal spine in a straight coronal line to the wall of the nasal cavity slightly posterior to the plane of the aperture. Just behind the margin the nasal cavity floor forms an elevated, posteroinferiorly inclined platform that reaches backwards into the nasal cavity for 9.5 before abruptly dropping down 4.5 to the incisive fossa. Surmounting this platform is a low, median crest running posteriorly from the anterior nasal spine. Lateral to the spine the platform is incised on each side by narrow, irregular, transverse grooves. The incisive fossa is a transversely elongate oval, measuring 7.0 × 3.5. Posterior to the fossa a strong nasal crest runs posteriorly for 20, gradually increasing in height as it reaches the posterior midline break at the M^2 level.

Palatal aspect (Fig. 5A). With a palatal index of 63%, the palate is fairly broad (endomolare-endomolare = 39.3) relative to its length (est. orale-staphylion = 62.5). Both internal and external alveolar margins progressively diverge from the midline as far posterior as M^2, beyond which point there is a slight narrowing of the palate to the rear (Tables 1 and 2). In occlusal aspect the dental arcade describes a broad, even parabola. The incisors and canines are set in a low curve continuous with that of the posterior arcade, but the incisor row itself is positioned only a short distance anterior to the bicanine line and is weakly arched, giving the front of the palate a slightly truncated appearance. The LI^2 and LC crowns are in interproximal contact; the reconstructed bilateral chord distance between the midpoints of these IP contacts (i.e., the breadth of the incisor row) is 33.5.

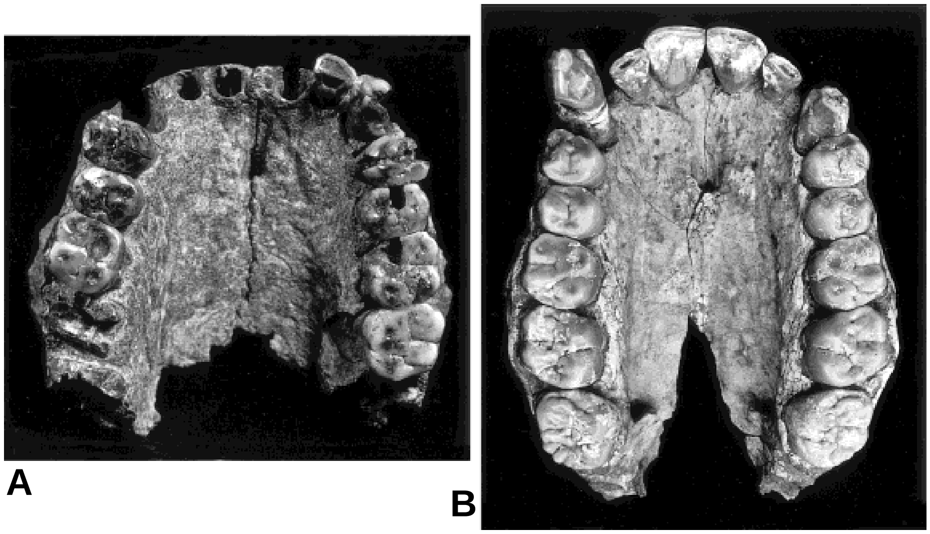

Fig. 5. Palatal views, A.L. 666-1 (**A**) and *A. afarensis* maxilla A.L. 200-1a (**B**). Seventy-six percent of natural size. See text for comparative discussion of palate and dental arcade shape.

TABLE 1. A.L. 666-1 bi-alveolar process breadth measurements

Position	Internal breadth	External breadth
C	30.3	—
C/P3	32.0	—
P3	33.0	—
P3/P4	36.2	57.7
P4	36.2	61.4
P4/M1	38.3	63.5
M1	38.5	(67.1)
M1/M2	38.5	67.5
M2	(39.3)	(69.5)
M2/M3	(39.0)	67.0
M3	(35.0)	(65.5)

Measurements in mm. Parentheses indicate estimates, ± 1.0 mm.

TABLE 2. A.L. 666-1 breadth between tooth crown faces

Position	Lingual	Buccal
P3	(35.0)	(59.0)
P4	36.2	61.0
M1	42.1	65.1
M2	(40.0)	(69.0)
M3	—	—

Measurements in mm. Parentheses indicate estimates, ± 1.0 mm.

TABLE 3. A.L. 666-1 palate depth measurements

Position	Measurement (mm)
P4	12.0
P4/M1	12.0
M1	14.5
M1/M2	16.5
M2	17.5
M2/M3	—
M3	—

At the level of the palate surface, the RI^2 alveolus is mesiodistally compressed (maximum width = 5.1), whereas the LI^1 alveolus is larger (maximum width = 6.5) and more circular in outline.

The palate is deep and strongly vaulted in coronal cross-section. Palatal depth increases posteriorly, with maximum measurable depth of 17.5 occurring at the M^2 level (Table 3). Posterior to the incisive foramen nearly vertical alveolar processes meet the palatine processes abruptly. Anterior to the incisive foramen the palate is markedly flexed inferiorly, the palatal surface sloping steeply to the alveolar margin throughout the anterior dental region (see Medial Aspect, above). The incisive foramen is centered opposite the P^3s; its posterior margin is located 21 from alveolare. It is 3.0 wide and opens into a well marked fossa that fans out towards the central incisor alveoli.

The most prominent features of the palate surface are strong grooves for the greater palatine nerves and vessels that follow the alveolar/palatine process junctions, hence

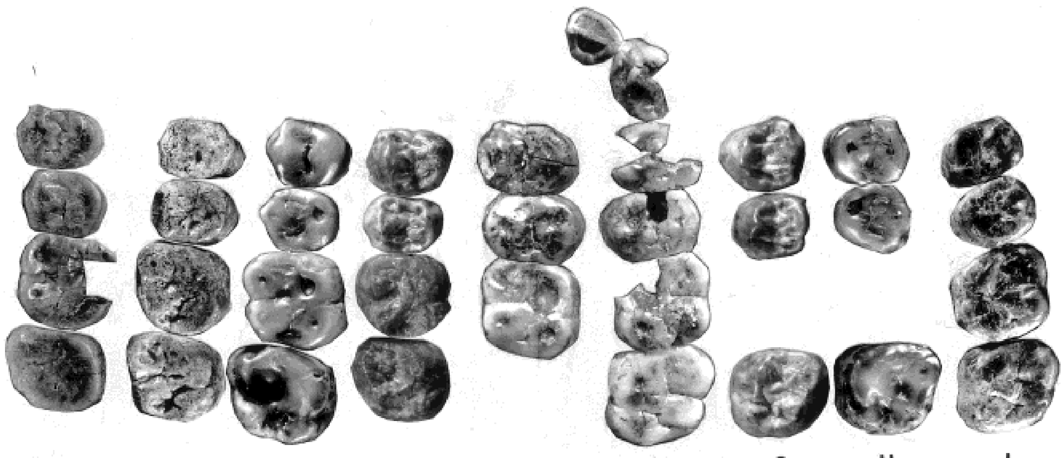

Fig. 6. Dental comparisons, A.L. 666-1 and *H. habilis*. **A:** L. 894-1 (RP^3-M^2). **B:** O.H. 13 (RP^3-M^2). **C:** O.H. 16 (RP^3-M^2). **D:** O.H. 39 (RP^3-M^2). **E:** A.L. 666-1 (RP^3-M^1). **F:** A.L. 666-1 (LI^2-M^2). **G:** O.H. 39 (LP^3, P^4, M^2). **H:** O.H. 16 (LP^3, P^4, M^2). **I:** KNM-ER 1813 (LP^3-M^2). Natural size.

demarcating the palate roof and separating it from its lateral walls, and then curve anteromedially to terminate on either side of the incisive foramen opposite the canines. Along their course these grooves give off a network of subsidiary sulci that descend the alveolar processes, sweeping anteroinferiorly toward the individual teeth.

Dentition (Figs. 5A, 6E,F; Table 4)

Lateral incisor (left). Although the mesiodistal crown diameter is greater than the labiolingual crown diameter, the basal outline of the complete left lateral incisor is a mildly mesiodistally compressed oval. Incisal wear is fairly advanced and exposes a 5.5 long, labially convex, distally tapering, cupped dentine strip. The incisal wear facet is planar but angles slightly disto-occlusally. The labial surface of the crown is quite flat vertically, weakly convex mesiodistally and features barely perceptible mesial and distal marginal ridges accompanied by correspondingly slight vertical grooves. The lingual surface is shovel-shaped, with a pronounced, bulbous basal tubercle. The lingual mesial and distal marginal ridges are thick, rounded shoulders set off from the featureless lingual fossa by deeply incised, vertical marginal grooves. The lingual marginal ridges coalesce with the basal tubercle and connect it to the incisal edge.

TABLE 4. A.L. 666-1 dental measurements

Position	Breadth (BL)	Length (MD)[1]	Crown area[2]	Crown shape[3]
LI2	7.0	7.4 (worn)	—	—
LC	—	[10.3]	—	—
LP3	—	8.6	—	—
LP4	12.6	8.3/9.0	113	71
LM1	—	12.0/13.0	—	—
LM2	14.4	12.4/13.5	194	94
RC	10.2	[10.4]	103	—
RP3	12.5	8.7/9.2	115	74
RP4	12.6	8.4/9.0	113	71
RM1	12.4	11.9/12.9	160	104

Measurements in mm. Bracketed figures are estimates (±0.2 mm) of true values on damaged teeth.
[1] For postcanine teeth, second mesiodistal length values are corrected for interproximal wear.
[2] Crown area = BL × MD (corrected), rounded to nearest mm^2.
[3] Crown shape = MD (corrected) × 100/BL, rounded to nearest per cent.

Canine (right and left). The canine crowns are fairly symmetric in occlusal, lingual and labial views. The occlusal outline is a labiolingually compressed oval. Occlusal wear, chiefly confined to the centrally located apex, perforates the enamel to create small, oval dentine exposures. Wear is more advanced and more nearly parallel to the postcanine occlusal plane on the right tooth than on the left, which shows mildly distolingually sloping wear and which continues to project below the occlusal plane of the neighboring teeth.

In labial and especially lingual views the canine appears as a blunt diamond, with

mesial and distal incisal edge components of subequal angulation and length and mesial and distal crown shoulders that strongly converge cervically above the interproximal contacts. The lingual face is divided into a small mesial and a slightly more extensive distal moiety by a low ridge set off by a distinct mesial furrow and a broader distal furrow. The furrows are bounded by blunt mesial and distal lingual marginal ridges that coalesce with a moderate gingival eminence. The labial face is marked by a weak mesial groove, a stronger distal groove, and correspondingly developed marginal ridges, lending the crown a slightly pinched appearance in occlusal view.

Third premolar (right and left). The P^3 crown outline is a mesiodistally compressed oval with a longer buccal half. On the right tooth, stepped, antemortem chippage extends from the apex of the paracone about half way up the buccal face of the crown; the buccal occlusal margin is a rounded, lingually convex shoulder delimiting the chip's extent on the occlusal surface. On the right tooth the mesial interproximal facet is deeply concave, actually indenting the mesial marginal ridge at the level of the occlusal surface.

The cusps, rounded by occlusal wear, appear low, bulbous and subequal in area and height. The paracone shows moderately developed mesial and distal wear slopes. The protocone of the right tooth bears a small dentine pit, whereas that of the left shows heavier wear forming a small oval exposure. The protocone's apex sits mesial of the crown's buccolingual midline and of the paracone. Anterior and posterior occlusal foveae are shallow; each is a transverse fissure intercepting a shallow median longitudinal groove that weakly separates the two cusps. The mesial marginal ridge is elevated. The buccal face is strongly convex both mesiodistally and occluso-apically, has a moderate, symmetric, basal bulge, and bears a moderate mesial buccal groove and a faint distal buccal groove. The lingual face is vertical. Both lingual and buccal enamel lines are straight, the latter lacking mesio-apical extension.

Fourth premolar (right and left). The occlusal outline is a mesiodistally compressed oval with a longer lingual dimension. The distolingual corner of the crown is weakly abbreviated; this is more evident on the right tooth. Overall, the P^4 is slightly smaller than the P^3. Occlusal wear is more advanced than on P^3, with larger dentine exposures on the apices of both buccal and lingual cusps. Lingual dentine exposures are larger than the buccal ones; this discrepancy is especially marked on the left tooth, where the protocone bears a 2.5 diameter, circular crater and dentine exposure. Occlusal wear forms mesial, distal and lingual slopes, although they are not strongly differentiated from one another. Mesial and distal interproximal wear facets reach the occlusal surface along their entire lengths.

Both cusps are bulbous in occlusal view. The protocone is larger than the paracone and is situated mesial of the latter and of the crown's buccolingual midline. A short, shallow segment of the anterior fovea is present on the right, just buccal to the crown's mesiodistal midline. It barely touches the relatively strong median longitudinal groove, which runs distally to link up with the better defined, transversely oriented and centered posterior fovea. Both the buccal and lingual faces are vertical. The buccal face has barely discernible mesial and distal furrows. The lingual and buccal enamel lines are straight.

Premolar root number. Damage to the external alveolar plates reveals that left P^3 and P^4 are two-rooted, with single buccal and lingual roots. The right P^4 also appears two-rooted. However, a shallow vertical groove divides the external surface of the right P^3 buccal root into a mesial component and a slightly smaller distal component. This groove commences about 2.0 above the enamel line and runs apically for 2.5 before disappearing beneath the buccal alveolar plate. It may indicate incomplete division of the right P^3 buccal root toward the root tip, but this will require direct confirmation by radiography.

First molar (left and right). The occlusal outline is a slightly mesiodistally

enlongate rectangle, which was even longer prior to the onset of interproximal attrition. Occlusal wear flattens the mesial cusps, but the distal cusps retain some apical topography. On the right tooth the protocone bears a deeply cupped, 3.5 diameter dentine exposure (this area is broken on the left, but traces of a similarly extensive dentine exposure are visible); the hypocone bears a smaller, cupped 1.6 diameter exposure, while the paracone and metacone display still smaller, subequal dentine pits. Mesial and distal interproximal facets reach the occlusal plane, but only the mesial facet extends the full breadth of the crown. The exposed right distal facet is 6.0 wide, flat at the occusal level, but further rootward is very weakly convex buccolingually.

Cusp area decreases in the sequence: protocone > metacone ≅ paracone > hypocone. The anterior occlusal fovea is all but obliterated by wear, but the posterior fovea is a deep, transverse incision in the distally extended distal marginal ridge. Remains of the median longitudinal groove occur just mesial to the buccal occlusal groove, which it intersects, and between the crista obliqua and the posterior fovea. The deep extensions of the occlusal grooves on the lingual and especially the buccal face give the crown's occlusal outline a pinched appearance. These grooves run vertically up the crown faces, becoming shallow furrows before reaching the enamel lines. The buccal face is bilobed but flat vertically, while the lingual face is slightly convex vertically. The buccal face features a basal bulge and groove, better developed on the paracone than on the metacone.

Second molar (left). The M^2 is larger and relatively broader buccolingually than the M^1. Its occlusal outline is a skewed rhomboid, with a distolingual to mesiobuccal slanting distal face and a truncated distobuccal corner. Occlusal wear flattens the protocone and polishes the mesial marginal ridge, largely obliterating the anterior fovea, but leaves the remaining three cusps with moderate apical topography and the distal marginal ridge mostly unscathed. The protocone bears a circular, 1.3 diameter dentine exposure. The slightly concave mesial interproximal facet is centered and reaches the occlusal level. The exposed distal facet just reaches the occlusal level, is 6.2 wide and slightly convex buccolingually.

Cusp area decreases in the sequence: protocone > paracone > metacone ≅ hypocone. Unlike the M^1, where the buccal cusps are aligned mesiodistally, the metacone sits lingual to the paracone on M^2. Only a tiny trace of the anterior fovea remains, just in front of the paracone. The slightly buccally displaced posterior fovea consists of a mesially concave, long and deep buccal arm that runs up behind the lingual slope of the metacone, and a shorter, shallower lingual arm, surmounting a strong distal marginal ridge. The median longitudinal groove traverses the shallow remains of what must have been a fairly open central fovea, intersecting both the buccal and the lingual occlusal grooves before entering the posterior fovea. The lingual occlusal groove, set well distal to its buccal counterpart, is deep near the central part of the occlusal surface but lingually shallows considerably (due to wear) before spilling over on to the lingual face of the crown as a short furrow that runs vertically about halfway toward the enamel line. The lingual face of the protocone bears a very shallow depression just below the occlusal enamel rim that may represent a Carabelli's feature. A deep and sharp buccal occlusal groove strongly notches the occlusal rim as it turns on to the buccal face, where it ends abruptly. The lingual face is mildly convex mesiodistally, but slightly more so vertically, whereas the buccal face is fairly flat both vertically and mesiodistally. A narrow, linear bulge and groove—especially well marked on the buccal and mesial faces—runs around the crown base. Lingual and buccal enamel lines are straight.

Age and sex. Dental occlusal and interproximal wear on LM^2 and both canines indicate that A.L. 666-1 was a full adult at death. Male attributes include inflated contours of the maxillary corpus and zygomatic process roots due to expansive maxillary sinus cavities, absolutely long palate, and a fairly large canine crown (crown base area = 106 mm^2) that, although apically flattened by occlusal wear, projects below the level of the

TABLE 5. Palate dimensions and shape index in early hominids

Specimen/taxon	Palate breadth	Palate length	Shape index	Comments
A.L. 417-1d (*A. afarensis*)	28.5	58.0	.49	Lg est.
A.L. 444-2 (*A. afarensis*)	41.0	75.0	.55	Lg + Br est.
A.L. 200-1a (*A. afarensis*)	33.5	65.0[4]	.52	Lg est.
A.L. 199-1 (*A. afarensis*)	32.0	54.0	.59	Lg est.
Sts. 53 (*A. africanus*)	32.0	54.0	.59	Lg + Br est.
Stw. 73 (*A. africanus*)	32.0	58.0	.55	Lg est.
Sts. 5 (*A. africanus*)	35.7	65.3	.55	
SKW 11[3] (*A. robustus*)	34.2	60.0	.57	Lg est. (cast)
O.H. 5[1] (*A. boisei*)	38.2	79.1	.48	
KNM-ER 406 (*A. boisei*)	37.4	70.0	.53	
KNM-ER 405 (*A. boisei*)	38.0	75.0	.51	Lg + Br est.
KNM-CH 1[1] (*A. boisei*)	40.8	72.0	.57	
KNM-WT 15000[2] (*H. erectus*)	40.0	59.0	.68	subadult
Sangiran 4[3] (*H. erectus*)	50.0	70.0	.71	Lg + Br est.
KNM-ER 3733[2] (*H. erectus*)	34.0	50.0	.68	
KNM-ER 1813 (*H. habilis*)	34.5	53.5	.65	
O.H. 24 (*H. habilis*)	35.5	50.7	.70	
A.L. 666-1	39.3	62.5	.63	Lg est.

Distance units = mm. Palate breadth (Br) is the bilateral distance between the midpoints on the internal margins of the M2 alveoli (Martin no. 63). Palate length (Lg) is the direct chord distance between the points orale and staphylion (Martin no. 62). Estimated distances are ±1.0 for breadth and ±2.0 for length.

[1] From Tobias, 1991.

[2] From Walker and Leakey, 1993.

[3] Measurement by the authors on a cast.

[4] Palate length value given here for A.L. 200-1a differs from that reported in Kimbel et al. (1982), where the figure of 57.0, erroneously recorded as "palate length" (Martin no. 62) is actually the "anterior maxillary palate length" (Martin no. 62-1). The figure provided here corresponds to Martin's no. 62.

occlusal plane of the neighboring teeth. These features are discussed in comparative context in the next section.

Comparative morphology of A.L. 666-1: *Australopithecus* vs. *Homo*

The collection of hominid upper jaws previously recovered from the Hadar Formation comprises a taxonomically informative part of the hypodigm of *Australopithecus afarensis*. This sample, recently and significantly expanded (Kimbel et al., 1994), is well known for its plesiomorphic (for hominids) combination of characters, including markedly protruding, sagittally and transversely convex nasoalveolar clivus; superomedially tapering midface; strong canine fossa; flat, shallow palate; long, narrow dental arcade; strongly arched anterior dental row; and buccolingually broad postcanine teeth (White et al., 1981; Rak, 1983; Kimbel et al., 1984, 1994). In each of these aspects A.L. 666-1 presents a derived condition that distinguishes it not only from *A. afarensis*, but also from all other *Australopithecus* species. Both maxillary and dental morphology tie the new Hadar specimen firmly to the genus *Homo*.

Palate shape. Data presented in Table 5 show that while estimated palatal length is not remarkable in A.L. 666-1, the palate is relatively broad compared to those of *Australopithecus*. *Australopithecus* palates that are approximately as long as that of A.L. 666-1 are much narrower (A.L. 200-1a [Fig. 5B], Sts. 5), whereas, in contrast, palates that are as broad as the new Hadar maxilla are much longer (e.g., the large, putative male, "robust" *Australopithecus* crania: OH 5, KNM-ER 405, KNM-ER 406, KNM-CH 1). Thus, no *Australopithecus* palate in the sample has a palatal index of greater than 59% (two small, probable female maxillae, A.L. 199-1 and Sts. 53), and the mean index value for the genus is 54%. The palatal index of the small measurable sample of early *Homo* maxillae averages much higher (67%). At 63% the index for A.L. 666-1 is closest to that of the Koobi Fora *H. habilis* cranium KNM-ER 1813 (65%). Neither the *Australopithecus* nor the *Homo* sample reveals obvious intrageneric, systematic patterning in the palatal index.

Palate depth and the palatal index. As can be seen in Figure 7, whereas the palatal

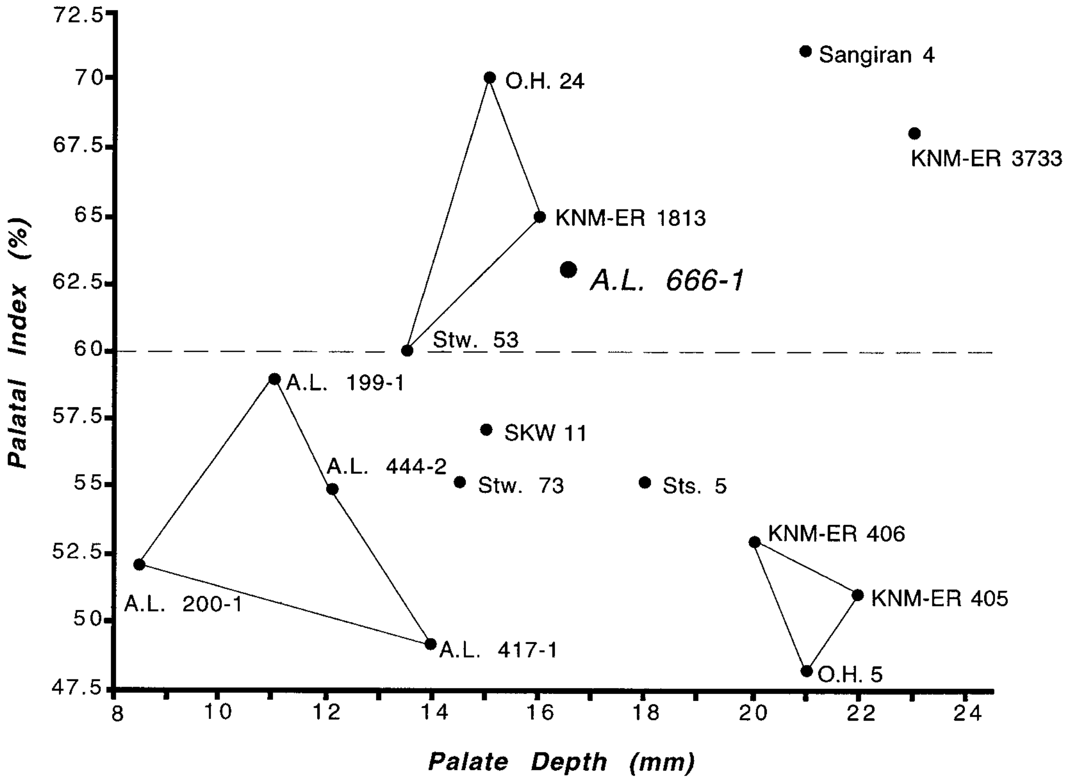

Fig. 7. Bivariate diagram of the palatal index (palate breadth/palate length × 100) plotted against palate depth measured at M^1/M^2. Polygons connect specimens in taxon hypodigms where $n > 2$ (lower left, *A. afarensis;* lower right, *A. boisei;* upper center, *H. habilis*).

index provides a useful guide for discriminating *Homo* from *Australopithecus* (note horizontal line in Figure 7), palatal depth does not. Only the very shallow palate of *A. afarensis* stands out among early hominids, providing a striking contrast with A.L. 666-1. On the other hand, the palates usually attributed to *H. erectus* are deeper than those of *H. habilis* with similar palatal shapes. Notably, A.L. 666-1 plots closest to the latter group.

Subnasal prognathism. Among hominids reduction of subnasal prognathism is a synapomorphy of *Homo*, whereas the subnasal region is primitively prognathic in *Australopithecus*. One way to express the verticality of the subnasal region in isolated maxillae is to compare the direct sagittal length of the nasoalveolar clivus (the nasospinale-prosthion length measured along the clivus's midsagittal contour) with its horizontal projected length; the ratio "projected length/direct length" is high in cases of marked horizontal inclination of the clivus and low where the clivus is relatively vertical. Data for A.L. 666-1 and other early hominids are presented in Table 6. In accord with expectation, the index values for *Australopithecus* maxillae are high, with species' sample means falling at or above 70%. (The fact that "robust" *Australopithecus* crania have a similar degree of subnasal prognathism to those of *A. africanus* and *A. afarensis*, yet generally show less total facial prognathism than the latter, is due in part to the retraction of the *entire* palate in the "robust" crania, as discussed by Rak (1983). Specimens such as OH 5, KNM-ER 406 and especially KNM-ER 405 remain highly prognathic subnasally.) Values for early *Homo* confirm the visual impression of subnasal verticality in this sample, with individual

TABLE 6. Relative subnasal prognathism in early hominid maxillae

Specimen/taxon	Pr-Ns proj. distance	Pr-Ns direct chord	Proj./ direct ratio
A.L. 444-2 (*A. afarensis*)	(25.0)	(33.0)	.76
A.L. 427-1 (*A. afarensis*)	23.5	30.0	.78
A.L. 200-1a (*A. afarensis*)	19.0	25.0	.76
Sts. 5 (*A. africanus*)	26.4	32.3	.82
Sts. 71 (*A. africanus*)	17.5	24.0	.73
Stw. 73 (*A. africanus*)	22.0	28.5	.77
Sts. 52a (*A. africanus*)	17.0	26.0	.65
SK 11 (*A. robustus*)	24.0	33.8	.71
SK 46 (*A. robustus*)	19.7	26.5	.74
SK 48 (*A. robustus*)	18.5	27.1	.68
SK 52 (*A. robustus*)	21.2	28.8	.74
SKW 11[3] (*A. robustus*)	21.5	30.7	.70
KNM-WT 17000[3] (*A. aeth.*)	26.5	31.5	.84
O.H. 5 (*A. boisei*)	30.0[1]	39.0[2]	.77
KNM-ER 3733 (*H. erectus*)	13.2	28.1	.47
SK 847 (*H. erectus*)	16.0	30.0	.53
Sangiran 4[3] (*H. erectus*)	18.0	29.0	.62
KNM-ER 1813 (*H. habilis*)	16.0	23.3	.69
O.H. 62 (*H. habilis*)	14.5	22.5	.64
KNM-ER 1470[1] (*H. rudolf.*)	31.7	36.0	.47
A.L. 666-1	20.0	32.0	.63

Distance units = mm. Projected horizontal distance prosthion-nasospinale vs. direct chord measured along the midsagittal contour of the nasoalveolar clivus. Parentheses indicate estimates, ± 1.0 mm.
[1] From Wood, 1991.
[2] From Tobias, 1967.
[3] Measurement on a cast taken by the authors.

values ranging from 47% to 69%. The A.L. 666-1 figure of 63% is less than that of any *Australopithecus* specimen in the sample, coming closest to the relatively orthognathic *A. africanus* maxilla Sts. 52a. It is, on the other hand, virtually identical in this respect to two specimens in the *Homo* sample, OH 62 and the Sangiran 4 maxilla.

Subnasal and nasal cavity morphology. Robinson (1953) was the first to recognize the taxonomic value of hominid nasal cavity variation in his comparative study of the SK 80 maxilla (now part of SK 847; Clarke, 1977). He drew attention to a suite of characters of the Swartkrans specimen that distinguish it from *Australopithecus,* in particular from *A. robustus,* with which SK 80 is contemporary in Member 1 of the Swartkrans deposit, and tie it to *Homo.* These include: 1) a broad, flat subnasal plane (nasoalveolar clivus) flexed at a strong, nearly acute, angle to the nasal cavity floor, from which it is demarcated by a distinct ridge (the *crista spinalis*); 2) elevation of the anterior part of the nasal cavity floor, which forms a horizontal platform situated between the *crista spinalis* and the nasal opening of the incisive canals; 3) insertion of the anterior tip of the vomer into the rear of the intranasal platform, resulting in a horizontal separation between the vomer and the anterior nasal spine. It is probable that the latter two characters are primitive within the hominids (they are present in *A. afarensis* and common in the African great apes) (Ward and Kimbel, 1983; McCollum et al., 1993). It is thus the modification of the primitively prognathic, convexly sloping nasoalveolar clivus, combined with the retention of primitive nasal cavity characters, that creates the distinctive morphology of the SK 847 maxilla.

In these respects, A.L. 666-1 bears a remarkable similarity to SK 847 (as can best be appreciated in midsagittal cross-section; see Fig. 8). The major difference between these specimens is that in SK 847 the anterior nasal spine occupies the most anterior point on the maxilla in a horizontal cross-section at the level of the inferior nasal margin, whereas in A.L. 666-1 the spinous tubercle (and the inferior nasal margin in general) is slightly recessed inside the nasal aperture. The nasal cavity topography of the Sangiran 4 maxilla, as well as of two early *H. erectus* crania, KNM-ER 3733 and KNM-WT 15000, shows strong similarities to that of A.L. 666-1 and SK 847 (see Fig. 8). (Sangiran 4 displays further synapomorphies within the *Homo* clade, shared in fact with *H. sapiens*: anterior nasal spine visible in true lateral view; anteriorly concave midsagittal profile of the nasoalveolar clivus superior to the incisor roots.) In fact, among early hominid maxillae only those of *Homo* species show the distinct *crista spinalis,* and the abrupt, sharply angled transition between the nasoalveolar clivus and the elevated intranasal platform separating the vomeral insertion from the anterior nasal spine, a combination that reaches full development in *H. sapiens.*

Most of the maxillae attributed to *H. rudolfensis* and *H. habilis* are to one degree or another damaged in the anterior part of the nasal cavity. The sole maxilla of the former taxon, KNM-ER 1470, is particularly poorly preserved here, but lateral to the midline there is clear evidence of a raised

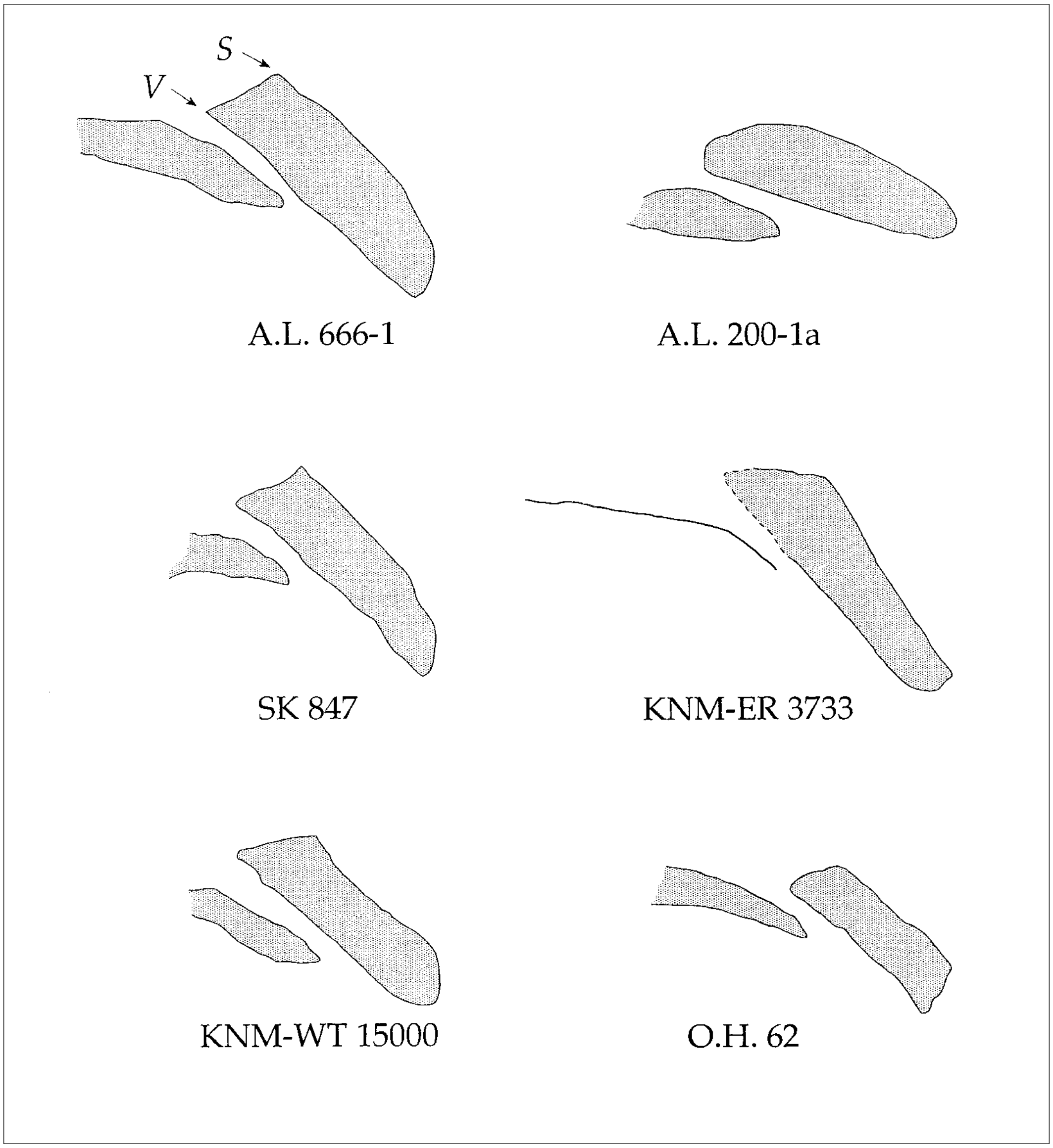

Fig. 8. Midsagittal sections of maxillae, illustrating nasoalveolar clivus and nasal cavity topography. For A.L. 666-1, V, vomeral insertion/incisive fossa; S, anterior nasal spine. Note contrast between *A. afarensis* maxilla A.L. 200-1a and the *Homo* specimens (see text for discussion). Natural size.

intranasal platform, and the transition between the flat, orthognathic subnasal plane and the floor of the nasal cavity is abrupt and sharply angled. Both OH 62 and Stw. 53 show an abrupt midsagittal transition between the nasoalveolar clivus and elevated intranasal platform, although the sagittal extent of the platform in these small (female?) *H. habilis* individuals is less (ca. 5.5–6.0) than in A.L. 666-1 (9.5) and the *H. erectus* maxillae (ca. 9.5–12.0) discussed above. *Homo habilis* specimen KNM-ER 1813 shows only a blunt *crista spinalis,* immediately behind which there is a sharp descent to the incisive fossa and the anterior vomeral insertion in the floor of the nasal

cavity. The latter configuration, which includes minimal overlap of the nasoalveolar clivus on the palatine process (as seen in sagittal cross-section), is the usual one in *A. africanus* (Robinson, 1953; Clarke, 1977; Ward and Kimbel, 1983; McCollum et al., 1993). No example of *A. africanus* demonstrates the suite of features described above for A.L. 666-1.

Division of the maxillary sinus. Examination of the now extensive series of *A. afarensis* maxillae from Hadar (n = 11) reveals a consistent pattern of partitioning of the maxillary sinus floor quite different from that observed in A.L. 666-1. In *A. afarensis* the sinus floor is divided into a large anterior chamber and a much smaller posterior chamber by a prominent transverse septum whose position relative to the tooth row varies between M^2/M^3 to distal M^3. Other less significant septa may subdivide the anterior chamber, but the chief division is always located far posteriorly in the sinus cavity. This pattern is clearly expressed in every Hadar *A. afarensis* maxilla in which the character can be judged: A.L. 199-1, A.L. 200-1a, A.L. 413-1, A.L. 427-1a, A.L. 442-1, A.L. 444-2, A.L. 486-1, and A.L. 651-1 (Fig. 4B). On the other hand, the division of the A.L. 666-1 sinus floor into a small anterior and a large posterior compartment by a strong crest running diagonally from the M^1/M^2 level posterolaterally to the P^4/M^1 level anteromedially is a configuration unknown in the Hadar *A. afarensis* sample (Fig. 4A). We were unsure what to make of this marked difference until we began to compare A.L. 666-1 to the maxillae of other hominid taxa, and found that specimens attributed to early species of *Homo* have precisely the same morphology as the new Hadar fossil. Thus, for example, in O.H. 62 and KNM-ER 1470 the maxillary sinus floor is prominently divided anteriorly. Breakage prevents assessment of the state of the posterior sinus floor in both of these specimens, but the presence of an anterior division is sufficient to distinguish them from *A. afarensis* and ally them with A.L. 666-1. The few casts of *A. africanus* maxillae in which the floor of the sinus cavity is exposed (MLD 9, MLD 45 [?], Stw. 73, Stw. 183 [a subadult]) definitely lack an anterior division, pointing to an *A. afarensis*–type pattern in this species. It is interesting to note, however, that several maxillae of *A. robustus* (SK 12) and *A. boisei* (KNM-ER 405, ER 733, ER 732[?]) seem to show the same anterior segmentation of the sinus floor as seen in the early *Homo* specimens. Confidence in the homology of the anterior dividing crest in *Homo* and "robust" *Australopithecus* is enhanced by their sharing the presence of the groove for the superior alveolar nerve and vessels on the summit of the crest (O.H. 62, KNM-ER 405, ER 733). In contrast, this sulcus travels along the lateral and anterior walls of the sinus cavity in *A. afarensis* (A.L. 199-1, A.L. 200-1a [Fig. 4B, vs. A.L. 666-1 in Fig. 4A], A.L. 427-1) and *A. africanus* (Stw. 183). Further research on the precise homologies and distribution of these characters in extant and fossil hominoids needs to be undertaken before definitive conclusions can be reached (our work, in prep.), but we tentatively suggest that the maxillary sinus floor morphology of A.L. 666-1 is inconsistent with a taxonomic attribution to *A. afarensis* or *A. africanus*. A host of other morphological information considered herein renders its assignment to a "robust" *Australopithecus* species most unlikely.

Facial morphology. In A.L. 666-1 the square maxillary profile—the absence of superomedial tapering of the midface in frontal view—strongly diverges from the generalized triangular maxillary profiles in *A. afarensis* and *A. africanus*. It is shared with many *Homo* specimens, such as KNM-ER 1805, OH 62, KNM-ER 3733, Sangiran 4 and SK 847. The square profile is accentuated in A.L. 666-1 and in the *H. erectus* specimens by flat maxillary plates alongside the nasal aperture, which face more anteriorly than laterally. In *H. habilis* this plate faces more laterally than in A.L. 666-1 and *H. erectus* counterparts (see O.H. 62, Stw. 53, KNM-ER 1813—but much less so in KNM-ER 1805, a putative male skull). In the single *H. rudolfensis* face (KNM-ER 1470), as in most *Australopithecus* specimens, the plate is directed almost completely anteriorly.

A second major point of similarity between A.L. 666-1 and some early *Homo* maxillae concerns the inflation or "smoothing" of facial contours in horizontal cross-section, due to the influence of a capacious maxillary sinus cavity. The forward extension of the maxillary sinus cavities to the coronal plane of the inferior nasal margin in A.L. 666-1 is uncommon, but is encountered in Sangiran 4, KNM-ER 1470 and KNM-ER 1805. Not all *H. habilis* or *H. erectus* crania show such an aggressive degree of maxillary sinus proliferation; it is not evident in KNM-ER 3733, OH 62, KNM-ER 1813 or Stw. 53, for example.

Essentially the same division of the early *Homo* sample occurs when we examine the facial contours of the maxilla. The faces of the second group listed above retain a generalized appearance (for hominids), with discrete "breaks" between maxillary contours (more extensive lateral maxillary surfaces and posteriorly positioned zygomatic process roots; i.e., a larger canine fossa). In this restricted sense, the morphology of the second group recalls the face of *A. afarensis* (Rak, 1983), in which the main maxillary sinus cavity reaches no further anteriorly than the incisive fossa, located at the rear edge of the intranasal platform separating the fossa from the inferior nasal margin. However, in those specimens with the most extensive maxillary sinuses: 1) there is only a small laterally directed interval of bone surface between the anterior maxillary surface and the root of the zygomatic process; 2) the zygomatic process appears to diverge gradually from the body of the maxilla in a smooth arc (in horizontal cross-section); and 3) the anterior edge of the heavily pneumatized zygomatic process is inflated forward over P^4.

These three characters can be summed together and expressed as the reduction in the distance between the coronal planes on which the middle and peripheral parts of the upper face are situated (compared to the generalized condition in the great apes and *A. afarensis*). Homologizing this character across taxa is not a straightforward matter, however, inasmuch as a similar compression of the distance between these coronal planes is apparently related to the great expansion of the maxillary sinus in some later *Homo* specimens (e.g., the Bodo cranium and Sangiran 17), on the one hand, but to reorganization of the masticatory apparatus in "robust" *Australopithecus* species, on the other hand. For present purposes the important point is that it is only in the *Homo* clade that this character manifests without elaboration of the masticatory apparatus, and, judging by the comparative dental morphology discussed below, this is certainly the case in the new Hadar maxilla.

Dental morphology. In most respects the dental anatomy of A.L. 666-1 follows a fairly conservative hominid pattern. Certainly, there are no indications of the highly derived dental apparatus typical of "robust" *Australopithecus* species. On the other hand, several of the primitive dental characters that distinguish *A. afarensis* from subsequent hominid species are modified in A.L. 666-1. The symmetric, buccolingually compressed, and apically worn maxillary canine of the new Hadar jaw represents a significant departure from the *A. afarensis* configuration, which is much more apelike (White et al., 1981; Johanson et al., 1982). In the same vein, the distinct, strongly inclined mesial and distal occlusal wear planes of the maxillary premolars and the persistent topographic disparity between the buccal and lingual cusps of occlusally worn upper molars, both so common in *A. afarensis* (White et al., 1981)—and expressed even in cases of fairly advanced wear (e.g., A.L. 333-1, A.L. 333-2, A.L. 417-1)—are not evident in A.L. 666-1. Although these dental characters permit A.L. 666-1 to be told apart from *A. afarensis,* they distinguish it much less efficiently from *A. africanus.* However, several features of the postcanine dentition do bolster the assignment of A.L. 666-1 to *Homo.*

A buccolingually broad M^1 crown is the standard, indeed, primitive, condition in *Australopithecus* (White et al., 1981; Leakey et al., 1995). The crown shape index (MD/BL) of 1.04 for the A.L. 666-1 M^1 indicates a significantly narrower tooth than in any *Australopithecus* species for which decent samples are available, with species' mean values falling in the .91–.92 range. On the other hand, the A.L. 666-1 tooth is a little

TABLE 7. Postcanine dental metrics for A.L. 666-1 and hominid reference taxa

	P³				P⁴				M¹				M²			
	$\bar{x}$	n	SD	r	$\bar{x}$	n	SD	r	$\bar{x}$	n	SD	r	$\bar{x}$	n	SD	r
A.L. 666-1																
MD	9.2	—	—	—	9.0	—	—	—	12.9	—	—	—	13.5	—	—	—
BL	12.5	—	—	—	12.6	—	—	—	12.4	—	—	—	14.4	—	—	—
Homo habilis																
MD	8.9	8	.4	8.2–9.4	9.1	9	.5	8.6–9.8	12.7	13	.8	11.5–13.6	13.0	7	.5	12.2–13.7
BL	11.4	7	1.1	9.3–12.7	11.8	8	.7	10.9–12.6	12.8	12	.6	11.9–13.8	14.3	8	1.1	13.1–16.0
Homo rudolfensis																
MD	10.3	1	—	—	10.7	1	—	—	14.1	1	—	—	14.7	1	—	—
BL	13.5	1	—	—	13.7	1	—	—	14.2	1	—	—	16.8	1	—	—
Homo erectus (early)																
MD	9.1	3	.4	8.7–9.5	8.1	2	—	8.1	12.8	4	.7	12.2–13.8	12.6	4	.9	11.8–13.8
BL	12.3	3	.9	11.7–13.3	11.9	2	—	11.7–12.1	13.1	3	.8	12.2–13.3	13.5	4	1.0	12.4–14.8
Homo erectus (late)																
MD	8.3	4	.8	7.4–9.2	8.0	8	.7	7.2–8.9	11.4	6	1.1	10.0–13.1	11.0	6	.7	10.3–12.2
BL	11.9	4	1.1	10.5–12.8	11.4	8	.7	10.3–12.5	12.6	5	.9	11.7–13.4	12.7	6	.6	12.2–13.4
A. afarensis																
MD	8.7	9	.5	7.5–9.3	9.1	17	.7	7.6–10.8	12.2	14	1.0	10.5–13.8	13.0	10	.6	12.1–14.1
BL	12.4	9	.6	11.3–13.4	12.4	11	.8	11.1–14.5	13.4	12	.9	12.0–15.0	14.7	11	.6	13.4–15.8
A. africanus																
MD	9.0	14	.3	8.7–9.6	9.4	21	.6	8.7–10.8	12.7	28	.7	11.1–13.8	14.0	24	1.1	12.6–16.4
BL	12.5	12	.5	11.7–13.2	13.0	16	.9	10.7–14.2	13.7	19	.7	12.9–15.7	15.7	24	1.2	13.7–18.3
A. robustus																
MD	9.9	21	.5	9.2–10.7	10.7	26	.6	9.5–11.9	13.3	25	.8	11.4–15.6	14.5	24	.9	12.8–15.8
BL	13.8	19	.9	11.6–15.2	14.9	23	1.0	12.3–16.3	14.6	19	.9	13.0–16.8	15.8	21	1.0	14.1–16.9

Distance units = mm. All data based on samples reported and discussed in White et al. (1981), *except: H. erectus* (early), augmented with KNM-WT 15000 (Walker and Leakey, 1993); *H. erectus* (late) = Zhoukoudian Lower Cave sample (Weidenreich, 1937); *A. afarensis*, augmented with teeth discovered at Hadar, 1990–1994; *H. habilis*, augmented with O.H. 62 (Johanson et al., 1987). Mesiodistal lengths are corrected for interproximal wear in all cases, except the Zhoukoudian sample. The *H. rudolfensis* sample = KNM-ER 1590; *H. erectus* (early) = KNM-ER 807, 1808, 3733, KNM-WT 15000, SK 27; *H. habilis* = O.H. 13, 16, 21, 24, 39, 41, 44, 45, 62, KNM-ER 1805, 1813, Stw. 53, L. 894-1.

TABLE 8. Crown shape indices (mesiodistal length/buccolingual breadth) for A.L. 666-1 and hominid reference taxa

	P³				P⁴				M¹				M²			
	$\bar{x}$	n	SD	r	$\bar{x}$	n	SD	r	$\bar{x}$	n	SD	r	$\bar{x}$	n	SD	r
A.L. 666-1	.74	—	—	—	.71	—	—	—	1.04	—	—	—	.94	—	—	—
Homo habilis	.78	7	.08	.70–.95	.78	8	.02	.75–.79	1.00	12	.02	.96–1.04	.92	7	.04	.88–1.01
Homo rudolfensis	.76	1	—	—	.78	1	—	—	1.00	1	—	—	.88	1	—	—
Homo erectus (early)	.74	3	.02	.71–.76	.71	2	—	.67–.74	.98	3	.07	.91–1.04	.93	4	.04	.88–.98
Homo erectus (late)	.70	4	.01	.69–.72	.70	8	.03	.66–.75	.88	5	.06	.81–.97	.87	6	.08	.79–1.00
A. afarensis	.71	9	.03	.66–.74	.73	11	.04	.66–.81	.92	11	.06	.85–1.04	.88	10	.03	.84–.91
A. africanus	.73	12	.04	.67–.78	.73	16	.04	.66–.81	.92	17	.05	.80–1.00	.92	18	.05	.84–.99
A. robustus	.71	17	.04	.66–.84	.71	20	.03	.65–.77	.91	20	.05	.82–.99	.91	22	.05	.82–.99

All data based on samples reported and discussed in White et al. (1981), *except: H. erectus* (early), augmented with KNM-WT 15000 (Walker and Leakey, 1993); *H. erectus* (late) = Zhoukoudian Lower Cave sample (Weidenreich, 1937); *A. afarensis*, augmented with teeth discovered at Hadar, 1990–1994. Mesiodistal lengths are corrected for interproximal wear in all cases, except the Zhoukoudian sample. The *H. rudolfensis* sample = KNM-ER 1590; *H. erectus* (early) = KNM-ER 807, 1808, 3733, KNM-WT 15000, SK 27; *H. habilis* = O.H. 13, 16, 21, 24, 39, 41, 44, 45, KNM-ER 1805, 1813, Stw. 53, L. 894-1.

narrower than the mean for *H. habilis* (1.00) and for the small African *H. erectus* sample (.98) (see Tables 7 and 8).

In A.L. 666-1 the asymmetric, rhomboidal occlusal outline of the M^2 crown recalls Brown and Walker's (1993) description of early African *H. erectus* M^2s (e.g., KNM-ER 3733, WT 15000, ER 807). However, we would extend their characterization to the early African *Homo* sample as a whole, as it appears to apply to almost all known *H. habilis* M^2s (O.H. 13, O.H. 16, O.H. 39, L. 894-1, KNM-ER 1813, and, despite damage, undoubtedly O.H. 62 as well, but *not* Stw. 53; see Fig. 6 and also Tobias, 1991) as well as to the only known M^2 of *H. rudolfensis* (KNM-ER 1590). Although a rhomboidal M^2 crown shape is not unknown in *A. afarensis* (e.g., A.L. 444-2) and *A. africanus* (e.g., Sts. 8), a squarer, more symmetric occlusal out-

line tends to be the rule in these taxa, as in "robust" *Australopithecus* species.

A suite of maxillary premolar characters serve, in combination, to distinguish A.L. 666-1 from *A. afarensis* and *A. africanus*. The P^3's vertical lingual face, elevated mesial marginal ridge, buccal face basal symmetry, straight buccal enamel line, and lack of strong mesial buccal groove; and P^4's vertical lingual and buccal faces and hint of distolingual crown abbreviation create a morphological pattern closest to that of the "early *Homo*" sample in Suwa's (1990) detailed study.

Raw "cuspal" and "lateral" enamel thickness measures of naturally fractured surfaces on the moderately worn A.L. 666-1 LP^3 (CT = 1.52; LT = 1.35) and LM^1 (CT = 1.66) are much less than those recorded for "robust" *Australopithecus* postcanine teeth, but are within the range for East African *Homo* (see Beynon and Wood [1986] for method and comparative data). Our (unpublished) data on enamel thickness of comparably worn Hadar *A. afarensis* teeth likewise suggests relatively thin postcanine dental enamel for A.L. 666-1.

Taxonomic status at the species level

We assign the new Hadar maxilla A.L. 666-1 to the genus *Homo* based on the following combination of characters: 1) relatively broad palate; 2) mild subnasal prognathism; 3) flat nasoalveolar clivus sharply angled to floor of nasal cavity; 4) intranasal platform horizontally separating anterior nasal spine from vomeral insertion and incisive fossa; 5) anterior division of the maxillary sinus floor; 6) deep, square anterior midfacial profile; 7) anteroposterior compression of upper facial coronal planes related to aggressive maxillary sinus; 8) mesiodistally elongate M^1; 9) rhomboidal shape of M^2; and 10) thin postcanine tooth enamel

To *which* early species of *Homo* should A.L. 666-1 be attributed is a more problematic question. With the possible exception of palate depth, none of the characters we have discussed in support of the generic assignment of A.L. 666-1 affords a clear-cut taxonomic division within the early *Homo* sample. This is partly caused by variation within the boundaries of conventionally delineated taxa, partly by very small sample sizes for some taxa (*H. rudolfensis*, early *H. erectus*), and partly, but most importantly, by the fact that most of the characters that bear on the taxonomy of the Hadar specimen appear to be apomorphic for the *Homo* clade as a whole (and thus are useless as phylogenetic markers within it). Alternative taxonomic assignments for A.L. 666-1 are discussed below, in order of what we consider to be increasing likelihood.

Homo erectus. Comparisons of the new Hadar maxilla with the "early African *H. erectus*" (EAHE) sample are difficult due to the small number of well preserved specimens included in this group. Dental metric comparisons (Table 9) reveal that A.L. 666-1 falls within the EAHE size range in all postcanine positions save P^4 length and breadth, for which the EAHE sample consists of two dentally small individuals (KNM-ER 3733, WT 15000). However, it is in large part due to the inclusion in the EAHE sample of Swartkrans Member 1 cranium SK 27 (following Clarke, 1977) that this sample's range of variation expands upwards to capture the measurements for the A.L. 666-1 P^3 length and breadth, M^1 length, and M^2 length and breadth (SK 27 does not preserve P^4). A comparison with only the East African specimens highlights the rather large dimensions of the A.L. 666-1 postcanine teeth, especially of the M^2 (Table 9). Still, KNM-ER 807, whose M^1 breadth defines the upper end of the sample range for this dimension, certainly signals the presence in the East African sample of larger postcanine teeth than is documented by KNM-ER 3733 or WT 15000. (Wood [1991] assigns KNM-ER 807 to *Homo* sp. indet., but we consider the specimen's reduced M^3, especially in mesiodistal length, to tip the scales in favor of its inclusion in the EAHE sample. See also Brown and Walker [1993].) The surviving mesial portion of the A.L. 666-1 right M^3 root has a buccolingual dimension of 14.6, which must represent a *minimum* trigon breadth for the crown. Trigon breadths for the M^1 (12.5) and M^2 (14.3) crowns are smaller. The trigon breadth for the KNM-ER 807 M^3 is 12.1, which is much smaller than

TABLE 9. Dental metric comparison of A.L. 666-1 with "Early African H. erectus" *sample*

	I2		C		P3		P4		M1		M2	
	MD	LL	MD	LL	MD	BL	MD	BL	MD	BL	MD	BL
A.L. 666-1	7.4w	7.0	(10.4)	10.2	9.2	12.5	9.0	12.6	12.9	12.4	13.5	14.4
KNM-ER 3733	—	—	—	—	9.1	12.0	8.1	12.1	(12.6)	—	12.6	13.5
KNM-WT 15000	8.4	8.5	9.6	10.2	8.7	11.7	8.1	11.7	12.2	12.2	12.2	12.4
KNM-ER 1808	—	—	—	—	—	—	—	—	—	—	11.8	(13.4)
KNM-ER 803	—	—	9.2	8.9	—	—	—	—	—	—	—	—
KNM-ER 807	—	—	—	—	—	—	—	—	(12.6)	(13.8)	—	—
SK 27	7.9	7.8	10.6	(10.7)	9.5	(13.3)	—	—	13.8	13.3	13.8	(14.8)

Data from sources as noted in legend to Table 7. Parentheses indicate estimates, ± 0.2 mm.

the estimate of 14.0 for the damaged M^2 crown (cast measurements). It appears that A.L. 666-1 may lack the M^3 reduction that characterizes the small EAHE sample (Brown and Walker, 1993).

There are only two maxillary lateral incisors in the EAHE sample (KNM-WT 15000, SK 27, both unworn), but both of these are a good deal larger than that of A.L. 666-1, especially in labiolingual breadth (Table 9). In both I^2 dimensions the EAHE specimens fall at the top of, or exceed, the range of variation for *H. habilis*, whereas the Hadar tooth lies comfortably within it (mesiodistal: $\bar{x} = 7.0$, s.d. = .8, r = 5.9–8.0, n = 5; labiolingual: $\bar{x} = 6.7$, s.d. = 1.0, r = 5.5–8.1, n = 5). Subequality of labiolingual and mesiodistal crown dimensions is a feature of EAHE I^2s matched in the similarly tiny sample from Zhoukoudian Lower Cave (n = 2, both unworn; Weidenreich, 1937): for the two EAHE I^2s the ratios of labiolingual breadth to mesiodistal length (LL/MD) are 99% and 101% and for both of the Zhoukoudian teeth it is 99%. By comparison, the *H. habilis* I^2 is usually a more slender tooth (LL/MD $\bar{x}$ = 95%, n = 5), as in *Australopithecus* (White et al., 1981). The ratio for the A.L. 666-1 incisor is 95%, and, in the unworn state, would probably have been a bit lower still.[1]

Several features of the maxillary premolars distinguish the EAHE sample from A.L. 666-1. First, the maxillary premolars in the EAHE sample are more homomorphic relative to the condition in A.L. 666-1. In both P^3 and P^4, the buccal half of the crown is longer mesiodistally than the lingual half (KNM-ER 3733, WT 15000); in A.L. 666-1 the buccal half is longer in P^3 while the lingual half is longer in P^4 (see Fig. 6E). The EAHE pattern is repeated in the Sangiran 4 maxilla, whereas the Hadar specimen has the condition observed in *H. habilis* (KNM-ER 1813, O.H. 39, and probably O.H. 13; in O.H. 16 the buccal half is longer in P^3, while buccal and lingual crown lengths are equal in P^4) and *H. rudolfensis* (KNM-ER 1590), which is ubiquitous in *Australopithecus*. Noting the relatively large lingual cusp on *H. habilis* P^4s from Olduvai Gorge, Tobias (1991: 627–629) refers to the "moderate heteromorphy" of this taxon's maxillary premolars. Second, a strong, transverse enamel ridge connects the buccal and lingual cusps in EAHE maxillary premolars (Brown and Walker, 1993). This ridge may be responsible for the fact that both of the occlusally worn premolars of KNM-ER 3733 develop distinct, strongly inclined mesial and distal wear planes (here, too, the Sangiran 4 maxilla reiterates the EAHE morphology). In contrast, the premolars of A.L. 666-1 are more smoothly and roundly worn occlusally (Fig. 6E), even though the overall degree of wear in the Hadar specimen and ER 3733 is similar. The Hadar maxilla and *H. habilis* specimens O.H. 13, O.H. 16 and KNM-ER 1813 show comparable occlusal wear features on their maxillary premolars (Fig. 6), which are common in *A. africanus* as well (but not in *A. afarensis*; see above).

The A.L. 666-1 palate is slightly longer relative to breadth (by 5%) than the two

[1]The variation in the I^2 labiolingual/mesiodistal index is large in *H. habilis* (range = 87–106%; standard deviation = 7.1). However, this reflects the incisally worn condition of three teeth in the sample of five (i.e., KNM-ER 1813, KNM-ER 1805, O.H. 16), which effects a reduction in the mesiodistal length of the crown and an inflation of the index value. Thus, index values of 92% for ER 1813, 93% for ER 1805 and 106% for O.H. 16 must be considered *overestimates* of the values for the teeth in the unworn state. We can infer from this that the actual contrast between *H. habilis* and *H. erectus* is larger than the available samples indicate.

palates of EAHE (Table 5), but only one of the latter is fully adult (KNM-ER 3733, a probable female). However, the depth of the A.L. 666-1 palate is much less than that of KNM-ER 3733, falling instead with the relatively wide but shallower palates of *H. habilis* (Fig. 7). In relative subnasal prognathism (measured as described above; Table 6) the EAHE sample, here represented by SK 847 and KNM-ER 3733, demonstrates a more vertical nasoalveolar clivus than does A.L. 666-1 (whose prognathism index value exceeds the values for the EAHE specimens by 16% and 10%, respectively). In addition, in contrast to the Hadar maxilla, but similar to ER 1470, the nasoalveolar clivus in SK 847 and ER 3733 fails to project beyond the canines in lateral view. Although the subadult West Turkana EAHE cranium KNM-WT 15000 is more prognathic than either of the adult specimens (Walker and Leakey, 1993), the nasoalveolar clivus appears to undergo a ventral “rotation” with growth in this group, producing a more orthognathic condition in adults (Richtsmeier and Walker, 1993).

The strongest phenetic similarity between A.L. 666-1 and specimens of EAHE is found in the nasal cavity relationships, particularly in the marked angle between the nasoalveolar clivus and the elevated anterior part of the nasal floor (Fig. 8). However, as we have mentioned above, KNM-ER 1470, though damaged, also appears to have this configuration, as do some of the smaller *H. habilis* maxillae (O.H. 62, Stw. 53), though in a diminutive state, perhaps consistent with their female status.

Homo rudolfensis. Discovery of this taxon’s phylogenetic identity grew out of unease over the degree and especially the pattern of variation in the species *H. habilis*, under which the *H. rudolfensis* hypodigm was formerly subsumed. The most detailed examination of the taxon emphasizes *Homo*-like features of the neurocranium and a “masticatory anatomy comprising either retained primitive features or features that are homoplasic or apomorphies shared with the ‘robust’ australopithecines” (Wood, 1991: 273). *Homo rudolfensis* maxillary and maxillary dental morphology is available only on single specimens (the edentulous face of KNM-ER 1470 and the face-less dentition of KNM-ER 1590), which, however, differ from the morphological pattern described for A.L. 666-1.

Despite an expansive maxillary sinus antrum and the anteroposterior compression of the coronal planes of the face referred to earlier, A.L. 666-1 does not show the extreme foreshortening of the ER 1470 subnasal region—which fails to project anterior to the canines in lateral view—nor any evidence of the marked relative advancement of the peripheral face—in which the anterior surface of the maxillary zygomatic process resides on virtually the same coronal plane as the nasal aperture and the inferior root of the process is shifted forward over the premolars—that make the Koobi Fora specimen so distinctive (and so similar to “robust” *Australopithecus*, at least superficially: Rak, 1987; Bromage et al., 1995; Lieberman et al., 1996). A further difference between ER 1470 and A.L. 666-1 is found in the topography of the zygomatic process take-off (in horizontal cross-section just below the level of the inferior nasal margin). In the *H. rudolfensis* specimen the anterior face of the zygomatic process leaves the body of the maxilla at a right angle, projecting straight out to intersect the posterior face of the process in an asymmetric triangle whose apex falls at the level of P^4/M^1. This is similar to the configuration in many *A. africanus* specimens (see, for example, MLD 9 or Sts. 17). In the Hadar maxilla, as already described, the take-off of the zygomatic process root is gradual, and the meeting of the “anterior” and “posterior” faces of the root, although imperfectly preserved, can be reconstructed as more symmetric and located well posterior (at the level of distal M^1) to the initial take-off point of the process.

Dentally, KNM-ER 1590 has a very large maxillary canine (it is clearly from a male individual), both absolutely and relative to the size of P^3 (C/P^3 crown area ratio = 102%, compared to 92% for A.L. 666-1 and a mean of 83% for *H. habilis* [Table 10]). Yet, the ER 1590 P^3 itself is 21% larger in crown area than that of A.L. 666-1. The P^4 of ER 1590 is larger (by 5% of crown area) than its P^3, whereas in A.L. 666-1 P^3 is slightly larger than P^4 (Table 10). A P^3:P^4 crown area ratio

TABLE 10. Comparison of dental crown areas (mm^2) and crown area ratios (%) in A.L. 666-1 and early Homo *specimens*

	C area	P3 area	P4 area	M1 area	C/P3	C/M1	P3/P4	M1/M2
A.L. 666-1	103.0	115.0	113.4	160.0	87.8	63.1	101.4	82.3
KNM-ER 1813	71.4	96.9	99.2	152.5	73.7	46.8	97.7	86.4
KNM-ER 1805	84.8	95.9	94.6	174.2	88.4	48.7	101.4	100.1
O.H. 13	—	102.1	103.2	161.3	—	—	98.9	90.7
O.H. 16	91.3	112.8	115.9	187.7	80.9	48.6	97.4	87.8
O.H. 39	86.5	96.6	93.7	136.8	89.5	63.2	103.1	85.0
L. 894-1	—	116.8	117.1	180.9	—	—	98.9	102.5
H. habilis $\bar{x}$ (n)	83.5 (4)	103.5 (6)	104.0 (6)	165.6 (6)	83.1 (4)	51.8 (4)	99.6 (6)	92.1 (6)
KNM-ER 1590	141.5	139.1	146.6	200.2	101.7	70.7	94.9	81.1
KNM-ER 3733	—	109.2	98.0	—	—	—	111.4	—
KNM-WT 15000	97.9	101.8	94.8	148.8	96.2	65.8	107.4	—
SK 27	113.4	126.4	—	183.5	89.7	61.8	—	89.9
Sangiran 4	111.2	103.3	100.0	156.9	107.6	70.9	103.3	74.9
Z. D-I	89.2	—	—	132.2	—	67.5	—	93.5
Z. F-IV	109.2	117.8	—	—	92.7	—	—	—
Z. L-I	83.3	109.6	111.3	162.1	76.0	51.4	98.5	—
Z. L-II	—	77.7	78.8	117.0	—	—	98.6	88.8
Z. O-I	—	92.8	81.0	131.4	—	—	114.6	92.5

approaching or exceeding 100% is a primitive hominid character strongly expressed in *Australopithecus anamensis* specimen KNM-KP 29283 (Leakey et al., 1995) and, to a lesser degree, in *A. afarensis* (Garusi I and A.L. 200-1a), whereas in *A. africanus* and the "robust" *Australopithecus* species P^4 is almost always the larger premolar. A relatively large P^3 is also the rule in the early species of *Homo* (including Sangiran 4 and Zhoukoudian *H. erectus*), with the exception of the single *H. rudolfensis* individual, whose low P^3:P^4 ratio resembles the condition in the later *Australopithecus* species.

In its occlusolingually sloped buccal face the ER 1590 P^4 is more *Australopithecus*-like than A.L. 666-1 or *H. habilis* homologues, in which the P^4's buccal face is nearly vertical (see also Suwa, 1990). Finally, the three-rooted P^3s of ER 1470 and 1590 contrast with the ostensibly derived, two-root form of the A.L. 666-1 homologues, although, as several *H. habilis* P^3s retain the more complex three-root condition (e.g., O.H. 24, O.H. 62 and Stw. 53), upper premolar root form does not have much taxonomic valence within early *Homo* (see also Wood and Englemann, 1988; Tobias, 1991). These tooth size and proportional differences between ER 1590 and A.L. 666-1 stand in sharp relief given the probable male sex of both specimens.

Homo habilis. In most measurements of the palate A.L. 666-1 is larger than any maxilla in the hypodigm of this species (O.H. 13 [a subadult], O.H. 24, O.H. 62, KNM-ER 1813, ER 3891—which is remarkably similar in size and morphological detail to O.H. 62—and Stw. 53), with the probable exception of the badly distorted face of KNM-ER 1805, which, on visual evidence alone, is approximately the size of the Hadar specimen (Table 5). Palate breadth in A.L. 666-1 exceeds that of the *H. habilis* sample by about 14% ($\bar{x}$ = 34.4, n = 5, r = 32.0–35.5), but palate length is 20% greater than the mean value for only two *H. habilis* maxillae ($\bar{x}$ = 52.1, r = 50.7–53.5). Wood et al. (1991) have shown that intraspecific variation in palate dimensions (especially length) is a strong indicator of sexual dimorphism in the hominoids, and on this basis A.L. 666-1 cannot be ruled out as a suitable male counterpart to putative females such as ER 1813, O.H. 24, O.H. 62 and Stw. 53.

Similarly, the crown base area of the A.L. 666-1 canine falls above (by 16%) the upper extreme for four *H. habilis* homologs (Table 10), although this apparently is due to an unusually large mesiodistal diameter for the Hadar tooth, as two *H. habilis* canines, both probable males, have larger labiolingual dimensions than A.L. 666-1 (O.H. 15, on which extreme wear negates length measurement, and O.H. 16). All postcanine tooth dimensions for A.L. 666-1 fall within the *H. habilis* range, slightly above mean values except for the relatively narrow M^1, a relatively small

tooth overall (Table 7). Morphologically, the A.L. 666-1 postcanine teeth closely resemble those of *H. habilis* specimen O.H. 16 (the similarity between the M^1s is especially marked). In proportions along the toothrow, A.L. 666-1 shadows O.H. 39, a set of isolated teeth near the low end of the *H. habilis* size range from locality HWK EE in lower Bed II, Olduvai Gorge (Table 10). This is, again, consistent with an intraspecific pattern of variation based on sexual dimorphism in a taxon with small canines.

The only major postcanine dental feature of A.L. 666-1 that stands out against the attributes of the *H. habilis* sample is the absolutely and relatively broad P^4 crown (Fig. 6), the usual condition in *Australopithecus* (Tables 7 and 8) and the great apes. The A.L. 666-1 crown shape index of .71 falls more than three s.d. below the *H. habilis* mean. However, given the small sample size involved and the somewhat greater degree of variation within those hypodigms for which n exceeds 10, it would be imprudent to place great weight on the significance of this difference.

Facial morphology expected to have been present in the last common ancestor of the *Homo* clade is plentifully represented in the maxilla of *H. habilis*. The posterior origin of the zygomatic process; low, tightly curved zygomaticoalveolar crest; nasoalveolar clivus that projects (albeit weakly) anterior to the canines in lateral view; and the tendency (not universal) to elevate the anterior part of the nasal cavity floor—features that distinguish *H. habilis* from *A. africanus*—are probably hominid symplesiomorphies (Rak, 1983; Ward and Kimbel, 1983; Kimbel et al., 1984), but the relatively broad palate, moderately inclined subnasal region, and everted nasal aperture margins (achieved through lateral rotation of the frontal processes) surely are apomorphic for the genus *Homo* as a whole. On a character-by-character basis, there is, in fact, little in the face of *H. habilis* that is unique to this taxon. If, as seems reasonable, O.H. 24, O.H. 62, KNM-ER 1813 and Stw. 53 all represent females, then we must pursue the question of whether features that distinguish A.L. 666-1 from this group are attributable to sexual dimorphism. In this context the KNM-ER 1805 skull looms large, as it includes the best candidate for a male maxilla of *H. habilis* (Wood, 1991; Rightmire, 1993).

In this Koobi Fora maxilla, as in the Hadar specimen, the anterior face of the zygomatic process is inflated forward in association with an enlarged maxillary sinus, such that the horizontal distance between the anterior face of the zygomatic process and the plane of the nasal aperture is compressed, even though the inferior root of the zygomatic process maintains a relatively posterior position along the tooth row (above M^1/M^2). Even the detailed surface topography of this region in the ER 1805 maxilla matches that of A.L. 666-1: a marked vertical ridge above P^3 is all that separates the flat, anterolaterally directed maxillary surface from the anterior face of the zygomatic process, and the canine fossa is virtually absent. In the "female" group listed above, the zygomatic process and the plane of the nasal aperture are, in contrast, separated by a considerable topographic interval corresponding to the canine fossa, the generalized hominid morphology.

Whether this architectural difference qualifies as a "good" marker of sexual dimorphism is problematic if we employ extant hominoids as a guide, since what governs the morphology of this area in the faces of the great apes is the great size and robusticity of the male's canine root: if anything, the distance between the coronal planes of the nasal aperture and the zygomatic process is even greater in males than in females. Clearly, this aspect of great ape facial sexual dimorphism is an inappropriate model for those hominid taxa in which the canine roots are severely reduced (as also pointed out by Wood et al., 1991). On the other hand, for *A. boisei*, which has the smallest canines of any Plio-Pleistocene hominid, Rak (1983) has proposed that male faces (e.g., KNM-ER 406) differ from those of females (e.g., ER 732) in a fashion analogous to that under discussion here: the presence in ER 732 of a rudimentary "anterior pillar," due to the slightly greater offset between the anterior aspect of the zygomatic process and base of the frontal process, lends the female's facial anatomy a somewhat more generalized appearance (within the context of the su-

premely autapomorphic configuration of the *A. boisei* masticatory apparatus, of course!).

Yet, ER 1805 differs from A.L. 666-1 in at least one important respect, namely the degree and form of the subnasal prognathism. A strongly protruding, sagittally and transversely convex nasoalveolar clivus that arches smoothly into the nasal cavity is a primitively retained morphology of the Koobi Fora maxilla that recalls the condition in *A. afarensis*. This is, moreover, associated with a strongly curved anterior dental row featuring $I^2/\underline{C}$ diastemata. Although both A.L. 666-1 and ER 1805 have a nasoalveolar clivus that projects (weakly) anterior to the canines, the flatter clivus, strongly angled to the floor of the nasal cavity, and straighter anterior dental arch (in palatal view) are more derived features of the Hadar maxilla. Such sharp differences in subnasal morphology are not normally expected to distinguish individuals (especially of the same sex) within hominoid species. However, we must conclude with the observation that A.L. 666-1 strongly resembles other maxillae of *H. habilis* (i.e., O.H. 62, Stw. 53) in these respects, so perhaps it is the morphology of the Koobi Fora specimen that is unusual for the taxon.

DISCUSSION

The Hadar maxilla A.L. 666-1 clearly belongs in the *Homo* clade, but fails to satisfy a number of the fundamental diagnostic criteria of the currently recognized species of this clade. Among these species, the least likely attribution in our judgement is to the taxon that includes KNM-ER 3733 and WT 15000 (*H. erectus* [= *ergaster*]); dental features of A.L. 666-1 such as labiolingually compressed I^2, heteromorphic premolars, and inferred relatively large M^3 crown, plus the shallower palate and more inclined nasoalveolar clivus, argue against such an assignment. In each of these characters, it is the Hadar specimen that retains the more primitive state. The taxon represented by KNM-ER 1470 and ER 1590, *H. rudolfensis,* is also an unlikely destination for A.L. 666-1, although here caution is warranted owing to the miserably small samples available for comparison. Nevertheless, the Hadar maxilla clearly lacks the apomorphic remodeling of the subnasal region demonstrated in KNM-ER 1470. In addition, the advancement of the more peripheral parts of the maxilla in ER 1470 and the enlarged postcanine dentition (possibly including P^3 root complexity and steep P^3 to P^4 size gradient) in ER 1590, which raise questions concerning the cladistic affiliation of *H. rudolfensis* with the australopiths (e.g., Bromage et al., 1995; Lieberman et al., 1996), are not evident in A.L. 666-1. Of the presently recognized species of *Homo, H. habilis* is the least problematic allocation for A.L. 666-1, as many of the differences between the Hadar maxilla and specimens comprising the *H. habilis* hypodigm are reasonably attributable to intraspecific sexual dimorphism. Were we to accept Grine et al.'s (1993) suggestion that the Swartkrans *Homo* cranium SK 847 is appropriately assigned to *H. habilis* (see our caution on this point under Materials and Methods), then the allocation of A.L. 666-1 to this species might be reinforced based on the detailed similarity in the nasal cavity morphology of these two specimens; however, as discussed above, this similarity appears to be apomorphic for the entire *Homo* clade and thus would not be helpful in decisions at the species level. Still, the *H. habilis* taxonomic solution is also not without objections, namely the primitively broad P^4 in A.L. 666-1 and the primitive subnasal/anterior dental arch morphology of the putative male *H. habilis* maxilla KNM-ER 1805.

A broad view of the foregoing comparative summary reveals that, with the possible exception of this last character, A.L. 666-1 bears morphology that is arguably primitive for the *Homo* clade. On this basis, one could mount a logically appealing argument that the failure of the new Hadar maxilla to fit the diagnoses of any of the previously recognized species of *Homo* is tantamount to justifying the identification of a new one. We consider this a reasonable option, but in light of the deficiencies in the comparative base, as well as the possibility of recovering more hominid material at A.L. 666 or elsewhere in the Makaamitalu basin, we opt for a more conservative approach for the time being. Although we recognize the close phenetic relationship of the Hadar specimen to particular fossils in the hypodigm of *H.*

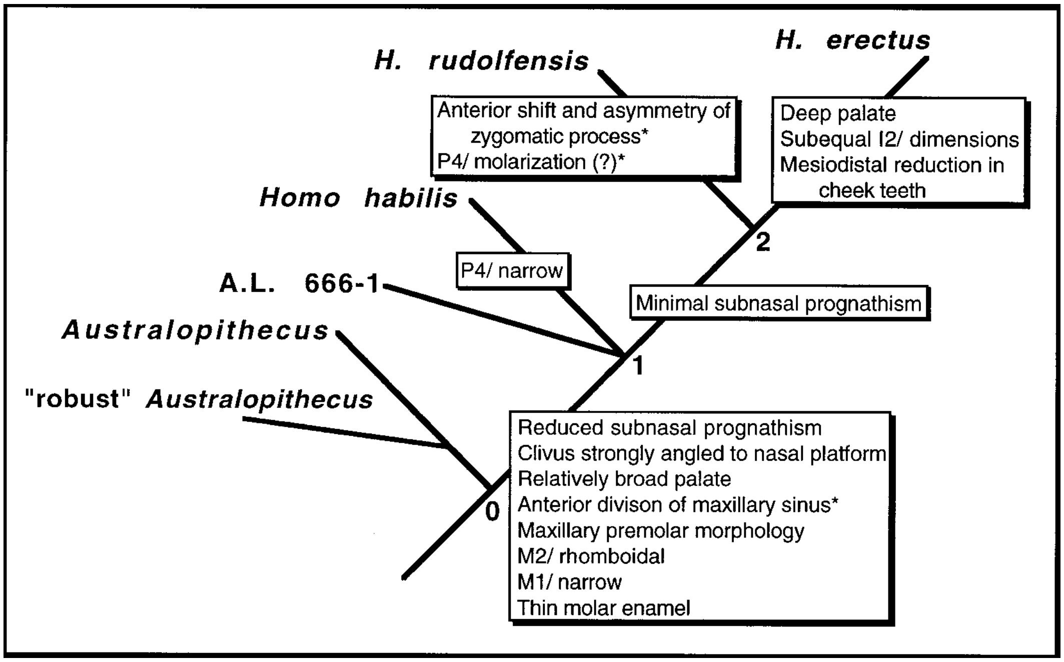

Fig. 9. Character phylogeny for features relevant to the systematics of the A.L. 666-1 maxilla. *Australopithecus* is taken to represent the ancestral condition at Node 0, although this taxon is probably paraphyletic and not all of its contained species share the same states for the characters listed. The characters acquired in the 0–1 internode are synapomorphic for *Homo*. The unresolved polychotomy at Node 1 reflects the strongly plesiomorphic condition of the Hadar specimen within the *Homo* clade. Characters bearing an asterisk are also present in one or more species of *Australopithecus* (see text for detailed discussion of these and all other listed characters).

habilis, this is based largely on the relatively high incidence of symplesiomorphic (within *Homo*) maxillary anatomy. This is itself sufficient reason to prefer caution. For the present, we assign A.L. 666-1 to *Homo* aff. *H. habilis,* cognizant that ongoing research may warrant revision of this conclusion at a later date.

With an age of 2.33 myr, the Hadar jaw's temporal locus lies within a poorly sampled period in the East African record of hominid evolution (Feibel et al., 1989; Kimbel, 1995). A.L. 666-1 is the oldest well-dated hominid fossil with strong morphological affinities to *H. habilis,* predating by ca. 400 kyr the stratigraphic (as opposed to phylogenetic) first appearance of this species in the Upper Burgi Member of the Koobi Fora Formation (e.g., KNM-ER 1813) and in the penecontemporaneous unit G-28 in the Shungura Formation (i.e., L. 894-1). That it shares chiefly primitive morphology with *H. habilis,* yet is in at least one aspect (P^4 shape) arguably more primitive than this taxon, is, from a phylogenetic point of view, consistent with its remote placement in time. In this regard it is noteworthy that among the 2.3–2.4 myr hominid premolars from the Shungura Formation affiliated by Suwa (1990) with post-2.0 myr *Homo* the sole complete P^4 shares with A.L. 666-1 a buccolingually broad crown compared with *H. habilis* (Omo 33-3282 from basal Member F, ca. 2.36 myr; shape index calculated from our corrected measurements of the original = .73; cf. Table 8). Should further sampling of pre-2.0 myr *Homo* continue to yield primitively broad P^4s, then the case for recognizing a distinct species for these hominids would be strengthened.

A secondary conclusion of this study is that of the species *H. habilis, H. rudolfensis* and *H. erectus,* it is *H. habilis* that appears to retain maxillary morphology closest to that expected in the hypothetical last com-

mon ancestor of the three (Fig. 9). This agrees with previous analyses of *H. habilis*'s phylogenetic relationships, based on craniodental hypodigms similar (but not identical) to the one used here (Chamberlain and Wood, 1987; Strait et al., 1997; but see Lieberman et al., 1996). The new Hadar maxilla is the first strong paleontological evidence for the projection of this primitive *Homo* palatofacial morphotype well back into the Pliocene.

So little is known about the Pliocene history of other early *Homo* species—whose existing African records are poor in any case—that little else can be concluded regarding the broader phylogenetic implications of the new Hadar maxilla. Each of several recent claims for the presence of early African *Homo* in the 2.0–2.5 myr temporal interval (Chemeron Formation: Hill et al. [1992]; Chiwondo Beds: Schrenk et al. [1993], Bromage et al. [1995]; Sterkfontein, Member 4: Kimbel and Rak [1993]) is beset by one or more uncertainties concerning provenience, dating or phylogenetic affinity. Thus, our view of early evolution in the genus *Homo* remains clouded. Ongoing field work in the upper units of the Hadar Formation may yet help to clarify the phylogenetic landscape by filling some of the remaining gaps in the crucial 2.0–2.5 myr zone.

ACKNOWLEDGMENTS

We thank the Center for Research and Conservation of Cultural Heritage (CRCCH) and the National Museum of Ethiopia, Ethiopian Ministry of Information and Culture, for their cooperation, assistance and permission to conduct field work at Hadar and laboratory research in Addis Ababa. We thank Gerald Eck, Erella Hovers, Charles Lockwood, Eric Meikle, Kaye Reed, Alan Walker, Bob Walter, Carol Ward, Bernard Wood for helpful discussion and/or assistance with comparative materials and data. Thanks are due Charlie Lucke for printing the photos in Figures 2–6. Critical comments by Fred Grine and an anonymous reviewer greatly improved the manuscript.

Thanks to the following members of the 1994 Hadar scientific team for their efforts during the recovery and initial excavation phase of work at A.L. 666: Gerald Eck, Kaye Reed, Rene Bobe, Million Haile Michael, Tesfaye Yemane, Bob Walter, Jim Aronson, Carl Vondra and Michael Tesfaye. We are grateful for the valuable assistance and advice of the CRCCH representatives to the 1994 Hadar project: Tamrat Wodajo, Tesfaye Hailu, and Ambachew Kebede. Special thanks to Ali Yesuf and Maumin Alahandu for finding the A.L. 666 hominid; to them, to the other Afar members of the field team, and to the people of Eloaha village we are, as always, indebted for exceptional friendship and assistance over many seasons of working and living together at Hadar.

LITERATURE CITED

Beynon AD and Wood BA (1986) Variation in enamel thickness and structure in East African hominids. Am. J. Phys. Anthropol. *70:*177–193.

Bräuer G (1994) How different are Asian and African *Homo erectus?* Cour. Forsch.-Inst. Senckenberg *171:* 301–318.

Bromage TG, Schrenk F, and Zonneveld FW (1995) Paleoanthropology of the Malawi Rift: An early hominid mandible from the Chiwondo Beds, northern Malawi. J. Hum. Evol. *28:*71–108.

Brown B and Walker A (1993) The dentition. In A Walker and R Leakey (eds.): The Nariokotome *Homo erectus* Skeleton. Cambridge, MA: Harvard University Press, pp. 161–192.

Chamberlain AT and Wood BA (1987) Early hominid phylogeny. J. Hum. Evol. *16:*119–133.

Clarke RJ (1977) The Cranium of the Swartkrans Hominid SK 847 and Its Relevance to Human Origins. Ph.D. thesis, University of the Witwatersrand, Johannesburg.

Clarke RJ (1994) The significance of the Swartkrans *Homo* to the *Homo erectus* problem. Cour. Forsch.-Inst. Senckenberg *171:*185–193.

Corvinus G (1976) Prehistoric exploration at Hadar, Ethiopia. Nature *261:*571–572.

Feibel CS, Brown FH, and McDougall I (1989) Stratigraphic context of fossil hominids from Omo Group deposits: Northern Turkana basin, Kenya and Ethiopia. Am. J. Phys. Anthropol. *78:*595–622.

Feibel CS, Harris JM, and Brown FH (1991) Paleoenvironmental context for the late Neogene of the Turkana basin. In JM Harris (ed.): Koobi Fora Research Project, vol. 3. The Fossil Ungulates: Geology, Fossil Artiodactyls and Paleoenvironments. Oxford: Clarendon, pp. 321–370.

Grine FE, Demes B, Jungers WL, and Cole T (1993) Taxonomic affinity of the early *Homo* cranium from Swartkrans, South Africa. Am. J. Phys. Anthropol. *92:*411–426.

Harris JWK (1983) Cultural beginnings: Plio-Pleistocene archaeological occurrences from the Afar, Ethiopia. In N David (ed): African Archaeological Review, vol. 1. Cambridge: Cambridge University Press, pp. 3–31.

Harrison T (1993) Cladistic concepts and the species problem in hominoid evolution. In WH Kimbel and LB Martin (eds.): Species, Species Concepts and Primate Evolution. New York: Plenum, pp. 345–372.

Hill A, Ward SC, Deino A, Curtis G, and Drake R (1992) Earliest *Homo.* Nature *355:*719–722.

Johanson DC and White TD (1979) A systematic assessment of early African hominids. Science *203:*321–329.

Johanson DC, White TD, and Coppens Y (1978) A new species of the genus *Australopithecus* (Primates: Hominidae) from the Pliocene of eastern Africa. Kirtlandia *28:*1–11.

Johanson DC, White TD, and Coppens Y (1982) Dental remains from the Hadar Formation, Ethiopia: 1974–1977 collections. Am. J. Phys. Anthropol. *57:*545–604.

Johanson DC, Masao FT, Eck GG, White TD, Walter RC, Kimbel WH, Asfaw B, Manega P, Ndessokia P, and Suwa G (1987) New partial skeleton of *Homo habilis* from Olduvai Gorge, Tanzania. Nature *327:*205–209.

Kimbel WH (1995) Hominid speciation and Pliocene climatic change. In ES Vrba, GH Denton, TC Partridge, and LH Burckle (eds.): Paleoclimate and Evolution, with Emphasis on Human Origins. New Haven: Yale University Press, pp. 425–437.

Kimbel WH and Rak Y (1993) The importance of species taxa in paleoanthropology and an argument for the phylogenetic concept of the species category. In WH Kimbel and LB Martin (eds.): Species, Species Concepts and Primate Evolution. New York: Plenum, pp. 461–484.

Kimbel WH, Johanson DC, and Coppens Y (1982) Pliocene hominid cranial remains from the Hadar Formation, Ethiopia. Am. J. Phys. Anthropol. *57:*453–499.

Kimbel WH, White TD, and Johanson DC (1984) Cranial morphology of *Australopithecus afarensis:* A comparative study based on a composite reconstruction of the adult skull. Am. J. Phys. Anthropol. *64:*337–388.

Kimbel WH, Johanson DC, and Rak Y (1994) The first skull and other new discoveries of *Australopithecus afarensis* at Hadar, Ethiopia. Nature *368:*449–451.

Kimbel WH, Walter RC, Johanson DC, Reed KE, Aronson JL, Assefa Z, Marean CW, Eck GG, Bobe R, Hovers E, Rak Y, Vondra C, Yemane T, York D, Chen Y, Evensen NM, and Smith PE (1996) Late Pliocene *Homo* and Oldowan tools from the Hadar Formation (Kada Hadar Member), Ethiopia. J. Hum. Evol. *31:* 549–561.

Leakey MG, Feibel CS, McDougall I, and Walker AC (1995) New four-million-year-old hominid species from Kanapoi and Allia Bay, Kenya. Nature *376:*565–571.

Lieberman DE, Wood BA, and Pilbeam DR (1996) Homoplasy and early *Homo:* An analysis of the evolutionary relationships of *Homo habilis sensu stricto* and *H. rudolfensis.* J. Hum. Evol. *30:*97–120.

McCollum MA, Grine FE, Ward SC, and Kimbel WH (1993) Subnasal morphological variation in extant hominoids and fossil hominids. J. Hum. Evol. *24:*87–111.

Rak Y (1983) The Australopithecine Face. New York: Academic.

Rak Y (1987) The unusual face of KNM-ER 1470. Résumés des Communications, Second Int. Congr. Human Paleontol., pp. 90–91 (abstract).

Renne PR, Walter RC, Verosub K, Sweitzer M, and Aronson J (1993) New data from Hadar (Ethiopia) support orbitally tuned time scale to 3.3 Ma. Geophys. Res. Lett. *20:*1067–1070.

Richtsmeier J and Walker AC (1993) A morphometric study of facial growth. In AC Walker and RE Leakey (eds.): The Nariokotome *Homo erectus* Skeleton. Cambridge, MA: Harvard University Press, pp. 391–410.

Rightmire GP (1991) The Evolution of *Homo erectus.* Cambridge: Cambridge University Press.

Rightmire GP (1993) Variation among early *Homo* crania from Olduvai Gorge and the Koobi Fora region. Am. J. Phys. Anthropol. *90:*1–34.

Robinson JT (1953) *Telanthropus* and its phylogenetic significance. Am. J. Phys. Anthropol. *11:*445–502.

Roche H and Tiercelin J-J (1977) Découverte d'une industrie lithique ancienne in situ dans la formation d'Hadar, Afar central, Ethiopie. C.R. Acad. Sci. Paris *2841:*1871–1874.

Schrenk F, Bromage T, Betzler C, Ring U, and Juwayeyi Y (1993) Oldest *Homo* and Pliocene biogeography of the Malawi Rift. Nature *365:*833–836.

Semaw S, Renne P, Harris JWK, Feibel CS, Bernor RL, Fesseha N, and Mowbray K (1997) 2.5-million-year-old stone tools from Gona, Ethiopia. Nature *385:*333–336.

Strait DS, Grine FE, and Moniz MA (1997) A reappraisal of early hominid phylogeny. J. Hum. Evol. *32:*17–82.

Suwa G (1990) A Comparative Analysis of Hominid Dental Remains from the Shungura and Usno Formations, Omo Valley, Ethiopia. Ph.D. thesis, University of California, Berkeley.

Tobias PV (1967) Olduvai Gorge, vol. 2. The Cranium and Maxillary Dentition of *Australopithecus (Zinjanthropus) boisei.* Cambridge: Cambridge University Press.

Tobias PV (1991) Olduvai Gorge, vol. 4. The Skulls, Endocasts and Teeth of *Homo habilis.* Cambridge: Cambridge University Press.

Walker AC (1993) Perspectives on the Nariokotome discovery. In AC Walker and RE Leakey (eds.): The Nariokotome *Homo erectus* Skeleton. Cambridge, MA: Harvard University Press, pp. 411–432.

Walker AC and Leakey RE (1993) The skull. In AC Walker and RE Leakey (eds.): The Nariokotome *Homo erectus* Skeleton. Cambridge, MA: Harvard University Press, pp. 63–94.

Walter RC (1989) Applications and limitations of fission-track geochronology to Quaternary tephras. Quaternary Int. *1:*35–46.

Walter RC (1994) Age of Lucy and the First Family: Single-crystal $^{40}Ar/^{39}Ar$ dating of the Denen Dora and lower Kada Hadar Members of the Hadar Formation, Ethiopia. Geology *22:*6–10.

Walter RC and Aronson JL (1993) Age and source of the Sidi Hakoma Tuff, Hadar Formation, Ethiopia. J. Hum. Evol. *25:*229–240.

Ward SC and Kimbel WH (1983) Subnasal alveolar morphology and the systematic position of *Sivapithecus.* Am. J. Phys. Anthropol. *61:*157–171.

Weidenreich F (1937) The dentition of *Sinanthropus pekinensis:* A comparative odontography of the hominids. Palaeontol. Sinica, new series D *1:*1–180.

White TD (1995) African omnivores: Global climatic change and Plio-Pleistocene hominids and suids. In ES Vrba, GH Denton, TC Partridge, and LH Burckle (eds.): Paleoclimate and Evolution, with Emphasis on Human Origins. New Haven: Yale University Press, pp. 369–384.

White TD, Johanson DC, and Kimbel WH (1981) *Australopithecus africanus:* Its phyletic position reconsidered. S. Afr. J. Sci. *77:*445–470.

Wood BA (1991) Koobi Fora Research Project, vol. 4. Hominid Cranial Remains. Oxford: Oxford University Press.

Wood BA (1993) Early *Homo:* how many species? In WH Kimbel and LB Martin (eds.): Species, Species Concepts and Primate Evolution. New York: Plenum, pp. 485–522.

Wood BA and Englemann CA (1988) Analysis of the dental morphology of Plio-Pleistocene hominids. V. Maxillary postcanine tooth morphology. J. Anat. *161:* 1–35.

Wood BA, Li Y, and Willoughby C (1991) Intraspecific variation and sexual dimorphism in cranial and dental variables among higher primates and their bearing on the hominid fossil record. J. Anat. *174:*185–205.